

American University in Cairo

AUC Knowledge Fountain

Theses and Dissertations

Student Research

2-1-2011

Direct detection of mycobacterium tuberculosis complex using gold nanoparticles

Marwa Mohsen Hussain

Follow this and additional works at: <https://fount.aucegypt.edu/etds>

Recommended Citation

APA Citation

Hussain, M. (2011). *Direct detection of mycobacterium tuberculosis complex using gold nanoparticles* [Master's Thesis, the American University in Cairo]. AUC Knowledge Fountain.

<https://fount.aucegypt.edu/etds/1314>

MLA Citation

Hussain, Marwa Mohsen. *Direct detection of mycobacterium tuberculosis complex using gold nanoparticles*. 2011. American University in Cairo, Master's Thesis. *AUC Knowledge Fountain*.

<https://fount.aucegypt.edu/etds/1314>

This Master's Thesis is brought to you for free and open access by the Student Research at AUC Knowledge Fountain. It has been accepted for inclusion in Theses and Dissertations by an authorized administrator of AUC Knowledge Fountain. For more information, please contact thesisadmin@aucegypt.edu.

The American University in Cairo

School of Science and Engineering



**DIRECT DETECTION OF MYCOBACTERIUM TUBERCULOSIS
COMPLEX USING GOLD NANOPARTICLES**

A Thesis submitted to
the Biotechnology Graduate Program

in partial fulfillment of the requirements for
the degree of Master of Science in Biotechnology

By Marwa Mohsen Hussain
Bachelor of Pharmaceutical Sciences

Under the supervision of
Prof. Hassan M. E. Azzazy

Fall 2011

The American University in Cairo

**Direct Detection of Mycobacterium Tuberculosis Complex Using Gold
Nanoparticles**

A Thesis submitted by
Marwa Mohsen Hussain

To the Biotechnology Graduate Program
Fall 2011

In partial fulfillment of the requirements for
the degree of Master of Science in Biotechnology

Has been approved by

Thesis Committee Supervisor /Chair Prof. Hassan M. E. Azzazy

Affiliation: Professor of the Chemistry department, School of Sciences and
Engineering, the American University in Cairo.

Thesis Committee Reader/Internal Examiner Dr. Wael Mamdouh

Affiliation: Associate Professor of the Chemistry department, School of Sciences and
Engineering, the American University in Cairo.

Thesis Committee Reader/ External Examiner Dr. Brent L. House

Affiliation: PhD, LCDR, MSC, U.S. Navy, Global Disease Detection and Response
Laboratory, U.S. Naval Medical Research Unit No. 3

Thesis Committee Reader/ External Examiner Dr. Wael Mostafa Tawakkol

Affiliation: Associate Professor and Chair of Microbiology department, Faculty of
Pharmacy, Misr University for Science and Technology.

Thesis Committee Observer Prof. Salah El Sheikh

Affiliation: Professor and Associate Chair of the Physics department, School of
Sciences and Engineering, the American University in Cairo.

Program Director

Date

Dean

Date

ACKNOWLEDGMENTS

I would like first to express my deepest and sincere gratitude to my advisor Prof. Hassan M. E. Azzazy (Professor at Chemistry department, School of Science and Engineering, The American University in Cairo) for his continuous support, help, and motivation through my Biotechnology Master Thesis study and research years. I profoundly appreciate his valuable and instructive comments during the process of writing. This thesis would not have been possible without his supervision and guidance throughout the whole practical and research work done. It is an honor for me to have him as an advisor.

My sincere thanks also go to my Biotechnology (AUC), Chemistry (AUC), and Microbiology (MUST) departments' colleagues who kept inspiring me through my academic years. Besides, I would like to express my sincere gratitude to Tamer Samir for his patience and assistance.

Last but not the least, I would like to thank my family who were always there for me.

Finally, I would like to acknowledge Misr University for Science and Technology (MUST), Faculty of Pharmacy, Microbiology department and the U.S. Naval Medical Research Unit No.3 (NAMRU-3) for supporting us with the mycobacteria strains' DNA and their collaborative support.

ABSTRACT

The American University in Cairo

DIRECT DETECTION OF MYCOBACTERIUM TUBERCULOSIS COMPLEX USING GOLD NANOPARTICLES

BY: Marwa Mohsen Hussain

Under the supervision of Prof. Hassan M. E. Azzazy

Tuberculosis (TB) is still one of the most significant causes of morbidity and mortality worldwide. According to WHO, TB causes 2 million deaths and more than 9 million new cases annually; the overwhelming majority of TB cases occur in developing countries where accurate diagnosis of TB remains a challenge. This work aims to develop a rapid nano-gold assay for specific detection of mycobacterium tuberculosis complex (MTBC). In the first version of the assay, DNA was extracted from clinical isolates grown on LJ media. 16s rDNA regions were amplified by PCR then the genus and species of MTB were confirmed by semi-nested PCR. Spherical gold nanoparticles (AuNPs; 13 nm) were synthesized by citrate reduction method of HAuCl₄ and characterized by spectrophotometry and SEM. In the first assay, the 16srDNA amplicons were denatured (95 °C, 30 s) then allowed to anneal (48 °C, 30 s) with genus- and species-specific oligotargeters in a hybridization buffer containing NaCl (40 nM). This was followed by the addition of unmodified AuNPs (14 nM). In case of a positive specimen, the AuNPs aggregated and the solution color changed from red to blue. The solution retained red color in case of negative specimen. This assay was further optimized to specifically differentiate MTBC from other mycobacterial strains. In the second version of the assay, MTBC was directly detected in the extracted genomic DNA. Species-specific oligotargeter was added to genomic DNA and denatured for 3 min at 95 °C followed by annealing at 48 °C for 1 min. AuNPs were added and solution color changed from red to blue in case of MTBC-positive specimens. The assay detection limit was 1 ng for PCR product and 40 ng for genomic DNA. The assay showed 100% sensitivity and specificity (n = 27) as compared with automated liquid culture system (MGIT) and semi-nested PCR. Following DNA extraction according to standard procedures, the assay turnaround time is about 1 hour. In conclusion, we have developed a nano-gold assay prototype for direct detection of MTBC as a low cost alternative to current amplification-based detection platforms. The developed assay is simple, sensitive, rapid, and shows a great potential in the clinical diagnosis of TB especially in developing countries with low resource settings.

TABLE OF CONTENTS

LIST OF TABLES.....	VIII
LIST OF FIGURES / ILLUSTRATIONS	IX
LIST OF ABBREVIATIONS.....	XI
CHAPTER 1: INTRODUCTION.....	1
CHAPTER 2: LITERATURE REVIEW	5
1. <i>Mycobacterium tuberculosis</i> bacteriology.....	5
2. <i>Mycobacterium</i> underlying problems.....	5
2.1. <i>Mycobacterium</i> species	5
2.2. <i>Mycobacterium</i> pathogenesis	7
2.3. <i>Mycobacterium</i> virulence and persistence factors	9
3. <i>Current Mycobacterium tuberculosis</i> diagnosis methods.....	9
3.1. Culture methods	9
3.2. Chromatography.....	10
3.3. Bacteriophage based method.....	11
3.4. Immuno diagnostics	11
3.5. Molecular techniques	12
3.5.1. Amplification	12
3.5.1.1. Target amplification	12
3.5.1.2. Probe amplification	13
3.5.1.3. Signal amplification	14
3.5.2. Electrophoresis based methods.....	14
3.5.3. Hybridization based methods	14
3.6. Sequencing.....	15
4. <i>Recent Mycobacterium tuberculosis</i> trends in diagnostic approaches	16
5. <i>Gold Nanoparticles</i>	17
5.1. Historic Background	17
5.2. AuNPs structure	18
5.3. AuNPs synthesis and Bio-conjugation.....	18
5.3.1. Synthesis.....	18
5.3.2. Bio-conjugation.....	19
5.4. Physicochemical properties.....	19
5.4.1. Absorbance properties	19

5.4.2.	Scattering properties.....	20
5.5.	Detection methods.....	20
5.5.1.	Non functionalized AuNPs.....	20
5.5.2.	Functionalized AuNPs.....	21
5.5.2.1.	Non cross-linking.....	21
5.5.2.2.	Cross linking.....	21
CHAPTER 3: MATERIALS AND METHODS.....		22
1.	<i>Mycobacteria strains</i>.....	22
2.	<i>Mycobacterial strains processing</i>.....	22
2.1.	Sample treatment.....	22
2.2.	DNA Extraction	22
2.3.	DNA quantification.....	23
3.	<i>Amplification of 16s rDNA gene segment</i>.....	24
3.1.	Primers design and analysis	24
3.2.	PCR.....	24
3.3.	Semi nested PCR.....	24
3.4.	PCR amplicons: Purification, visualization, and quantification.....	25
4.	<i>Gold nanoparticles synthesis</i>	25
5.	<i>TB nano-gold assay</i>	25
5.1.	Oligo-targeters selection	25
5.2.	Detection of TB PCR and genomic DNA	26
5.3.	Detection limit of TB nano-gold assay	26
CHAPTER 4: RESULTS		28
1.	<i>DNA extraction</i>.....	28
2.	<i>Amplification of 16s rDNA gene part</i>	28
2.1.	Primers design and analysis	28
2.2.	PCR.....	28
3.	<i>Gold nanoparticles synthesis</i>	29
4.	<i>TB nano-gold assay</i>	29
4.1.	Oligo-targeters selection	29
4.2.	Detection of TB PCR and Genomic DNA	29
4.3.	Detection limit of TB nanogold assay.....	30

CHAPTER 5: DISCUSSION	31
CHAPTER 6: CONCLUSIONS AND FUTURE PROSPECTS	37
CHAPTER 7: TABLES	38
CHAPTER 8: FIGURES	45
CHAPTER 9: REFERENCES.....	77

LIST OF TABLES

Table 1. Mycobacterium cell virulence factors exaggerating tuberculosis infection and persistence	38
Table 2. Commercial molecular techniques for detection of <i>Mycobacterium tuberculosis</i>	39
Table 3. Selected gold nanoparticles detection methods and their biological applications	40
Table 4. Mycobacterium strains used in this study	41
Table 5. PCR primers used for amplification of TB 16s rDNA	42
Table 6. Selected mycobacterium 16s rDNA specific oligo-targeters	43
Table 7. Concentrations of PCR products and digested genomic DNA	44

LIST OF FIGURES / ILLUSTRATIONS

Figure 1. WHO Tuberculosis incidence estimates in 2010	45
Figure 2. TB incidence, prevalence, and mortality rates in Egypt	46
Figure 3. Schematic representation of mycobacterial cell wall	47
Figure 4. Acid fast stain of mycobacterium cells	48
Figure 5. Mycobacterium tuberculosis infection: Three outcomes	49
Figure 6. The intracellular pathogenesis of mycobacterium infection	50
Figure 7. Immune factors affected by tuberculosis infection	51
Figure 8. Surface Plasmon Resonance (SPR) of gold nanoparticles	52
Figure 9. Optical properties of gold nanoparticles	53
Figure 10. Different methods for functionalization of gold nanoparticles	54
Figure 11. Agarose gel electrophoresis of extracted genomic mycobacterial DNA	55
Figure 12. Agarose gel electrophoresis of 16s rDNA amplified from mycobacteria reference and clinical strains	56
Figure 13. Agarose gel electrophoresis of 16s rDNA amplified from unidentified mycobacterium clinical strains	57
Figure 14. Agarose gel electrophoresis of genus- and species-specific amplicons prepared by semi-nested PCR from mycobacteria reference and clinical strains	58
Figure 15. Agarose gel electrophoresis of genus- and species-specific amplicons prepared by semi-nested PCR from unidentified mycobacteria clinical strains	59
Figure 16. Absorption spectra of synthesized spherical unmodified gold nanoparticles	60
Figure 17. NCBI nucleotide blast results of mycobacterium genus-specific oligo-targeter	61
Figure 18. NCBI nucleotide blast results of <i>M. tuberculosis</i> complex-specific oligo-targeter	62
Figure 19. Use of AuNPs for detection of PCR amplicons to differentiate mycobacterium genus from other bacteria	63
Figure 20. Use of AuNPs for detection of PCR amplicons to differentiate MBTC from mycobacterium genus	64
Figure 21. Use of AuNPs for detection of PCR amplicons to differentiate MBTC from mycobacterium genus	65

Figure 22. Use of AuNPs for detection of PCR amplicons to differentiate MBTC from mycobacterium genus	66
Figure 23. Absorption spectra of AuNPs used for detection of TB 16s rDNA amplicons	67
Figure 24. Use of AuNPs for detection of digested genomic DNA to differentiate mycobacterium genus from other bacteria	68
Figure 25. Use of AuNPs for detection of digested genomic DNA to differentiate MTBC from mycobacterium genus	69
Figure 26. Use of AuNPs for detection of <i>Bam</i> HI digested genomic DNA for 9 <i>M. tuberculosis</i> clinical specimens	70
Figure 27. Confirmation of AuNPs detection of <i>Bam</i> HI digested genomic DNA for 14 <i>M. tuberculosis</i> clinical specimens	71
Figure 28. Absorption spectra of AuNPs in samples containing mycobacteria digested genomic DNA	72
Figure 29. Nano-gold assay detection limit for <i>Mycobacterium H37Ra</i> PCR amplicons	73
Figure 30. Nano-gold assay detection limit for mycobacterium digested genomic DNA from clinical strains	74
Figure 31. Detection principle of unmodified gold nanoparticles	75
Figure 32. Possible hypothetical explanations for the use of a single, rather than two, oligo-targeter in the TB nano-gold assay	76

LIST OF ABBREVIATIONS

AuNPs: Gold Nanoparticles

BCG: Bacillus Calmette-Guérin

DMSO: Dimethyl Sulfoxide

dsDNA: Double Stranded DNA

ELISA: Enzyme Linked Immunosorbent Assay

GC: Guanine Cytosine

HIV: Human Immunodeficiency Virus

HPLC: High Performance Liquid Chromatography

iELISA: Indirect Enzyme Linked Immunosorbent Assay

IL: Interleukin

INF- γ : Interferon- γ

LAMP: Loop mediated isothermal amplification

LCR: Ligase chain reaction

LRP: Luciferase reporter phages

mAb: Monoclonal antibody

MDR: Multi-Drug Resistant

MSPQC: Multi-channel piezoelectric quartz crystal

MTB: *Mycobacterium tuberculosis*

MTBC: *Mycobacterium tuberculosis* complex

NPs: Nanoparticles

PBS: Phosphate Buffered Saline

PCR: Polymerase Chain Reaction

RE: Restriction Enzyme

rRNA: Ribosomal RNA

SDA: Strand Displacement Amplification

SERS: Surface Enhanced Raman Scattering

SPR: Surface Plasmon Resonance

SSCP: Single Stranded Conformational Polymorphism

ssDNA: Single Stranded DNA

TE: Tris-EDTA

Th: T-helper

WHO: World Health Organization

XDR: Extensive Drug Resistant

CHAPTER 1: Introduction

Tuberculosis (TB) affects one-third of the world's population and is a serious health problem worldwide. In 2010, *Mycobacterium tuberculosis* (MTB) infected about 8.8 millions [1]. The incidence of infection according to the World Health Organization (WHO) was estimated at 59 % in South East Asia, 26 % in African, 7 % in Eastern Mediterranean, 5 % in Europe, and 3 % in America. WHO estimated the rate of TB incidence to decline by < 1% per year (figure 1) [1]. TB global prevalence rate is 178 per 100,000 whereas mortality rate is 15 per 100,000 world's population which equals about 1.1 million deaths per year [1]. In Egypt, TB estimated incidence rate is 18 per 100,000, TB prevalence rate is 28 per 100,000 and mortality rate is 0.82 per 100,000 (figure 2) [2].

Several challenges hinder TB control efforts. First, TB is an airborne pathogen where each infected/untreated person is predicted to infect 10 - 15 persons per year. Second, TB also persists in the pulmonary cells in the lungs despite treatment. The treatment in most acute cases lasts for at least 6 months and patient compliance, assuming ability to tolerate side effects and cost, for this long period, is questionable [3-5]. This long treatment duration is mainly due to the thick mycobacterial cell wall structure which is rather complex and contains different long chain fatty acids (figure 3) [6]. What is more devastating is the relatively recent evidence that BCG "Bacillus Calmette-Guérin", the only available mycobacterium vaccine, has low efficacy that range from 0-80% depending on the immunized population [5]. The live attenuated vaccine lost its antigenic part region of difference (RD1) encoded proteins due to deletion mutation which stimulates the immunity to TB [5, 7]. This has led to decreased the immunization triggered and the variable efficacy range of 0% - 80% [3-5]. Low protection, due to lack of effective prophylactic vaccines, combined with malnutrition in developing countries augment disease progression [3-5].

In 2006, a strategic plan to control TB was developed jointly by WHO and the Stop TB organization (initiated in 2001 by different organization partnerships) [8]. The first goal of this strategy is to reduce TB prevalence and mortality rates by 50% (relative to 1990s rates) by year 2015. The second one is to get rid of TB infection as a public health concern by achieving an infection rate of 1 case per million by year

2050. All the six WHO regions are on their way to achieve 50% reduction of mortality and prevalence rates except for the African region. Incidence rates are also decreasing and are expected to meet the first goal of the Stop TB initiative in five WHO regions with the exception of South East Asia in which the incidence rate has not been reduced yet [8]. Stop TB program identified two key challenges to address TB diagnosis. The first challenge is improvement of current detection methods with a focus on developing sensitive and specific point of care testing (POCT) devices which could significantly contribute to TB detection. These devices are easily used, rapid, affordable, non- instrument dependant, and requires small volumes of reagents and samples. Patient's nearby testing also supports patient compliance [9, 10]. Another goal is the need for rule out tests. Rule out diagnosis is required for screening and epidemiology purposes and reducing number of patients who require complex investigations thus leading to best allocation of medical resources [10].

An ideal diagnostic assay for detection of the *Mycobacterium tuberculosis* must be sensitive with a low detection limit. It should detect *Mycobacterium* bacillus in early infection stages. It must be specific to detect the *M. tuberculosis* complex species. Besides, it should generate results fast to allow prompt initiation of treatment. The assay should not involve complicated procedures or sophisticated expensive equipments [4, 11-13]. Current TB detection methods involve smear microscopy, culture, and molecular techniques. Ziehl-Neelsen sputum staining depends on the ability of mycobacterium to resist acid de-colorization for its high mycolic acid content. It depends on visual microscopic examination. The method cannot detect some early and mid infections [14]. Culture method is considered the standard method for TB detection. However, it requires from 6 – 8 weeks to confirm MTB growth on Lowenstein Jensen (solid media) [4, 14-16]. BACTEC 460 is a $^{14}\text{CO}_2$ modified Middlebrook 7H12 automated detection system. The system detected mycobacterium respiration of ^{14}C isotope labeled palmitic acid [15]. The main disadvantages include the disposal of radioactive materials, high cost, and turnaround time of 5 – 10 days, and inability of this system to differentiate mycobacterium from non-mycobacterial species. This prevents the use of BACTEC 460 in rapid mycobacterium diagnosis [4, 14-16].

Molecular methods for detection of MTB include Cobas® AmpliCor. [17-19]. This PCR-based method detects MTB within 6.5 h with sensitivity from 91 – 100%. Another method, Gen-Probe® AMPLIFIED detects MTB in 3.5 h but with a reported 86.8% sensitivity [14, 17, 19]. Although molecular detection methods show high sensitivity and specificity, they are expensive, time consuming, require sophisticated laboratory infrastructure, and highly trained personnel. None of the commercially available TB tests qualifies as an ideal *Mycobacterium tuberculosis* diagnostic method for TB strain identification [4, 11-13].

How can these limitations be circumvented using nanoparticles (NPs)? NPs are 1-100 nm in size (where 1 nm = 10^{-9} m) [20, 21]. They have unique and diverse physical and chemical properties depending on the size, shape, and materials of which they are synthesized. They can be designed in various shapes such as spheres, tubes, rods, or cubes, and can be made from different materials either inorganic elements such as gold, carbon and semiconductors or organic materials such as liposomes and dendrimers [21, 22]. Nanoparticles allow almost one-on-one interaction with biological molecules such as enzymes, proteins, and nucleic acids, since they are in the nanometer size; which significantly enhances diagnostic sensitivity [23-25]. Additionally, nanoparticles can act as scaffolds as they have a large volume: surface area ratio. This could permit functionalizing NPs with over 100 small molecules and of about 30 oligonucleotide strands [26].

Gold nanoparticles (AuNPs) exhibit distinctive optical properties based on their size, shape, and surface charge [21, 23]. When an incident light, which has an electromagnetic oscillating field, has a wavelength smaller than the particles diameter, the nanoparticles induces a collective dipolar oscillation. This oscillation lies in the free conduction band electrons around the metal nanoparticles surface [23, 27, 28]. At specific frequency, the oscillation amplitude gets to the maximum. This frequency is known as Surface Plasmon Resonance (SPR) [27, 29-31]. Another closely related phenomenon is plasmon - plasmon interaction in which AuNPs aggregate together changing their color from red to blue. AuNPs can be induced to aggregate using electrolytes such as salt [23, 30]. AuNPs scattering optical properties are highly dependent on particle size. AuNPs 80 nm in size show light scattering 10^5 fold higher than other traditional fluorescent molecules [27, 31, 32].

In this study, unmodified spherical AuNPs were employed to develop a prototype test to detect *Mycobacterium tuberculosis* complex 16s rDNA gene sequence amplified from clinical samples. The first version of the developed assay detected MTB PCR products. A second optimized version was used to directly detect genomic DNA in clinical specimens. The assay employs an oligo-targeter sequence against a conserved region in the 16s rRNA gene of TB genome. Clinical performance characteristics of the assay including sensitivity, specificity and detection limit were calculated using MTB PCR products and genomic TB DNA obtained from clinical isolates.

CHAPTER 2: Literature review

1. *Mycobacterium tuberculosis* bacteriology

Tuberculosis is an airborne respiratory disease. It spreads, in 95% of cases, through cough, sneezing, and sputum droplets. TB is caused by a bacterium termed *Mycobacterium tuberculosis* (MTB) which is an acid-fast beaded bacilli, non motile, non-spore forming, straight or slightly curved rods (figure 4) [33].

Microscopically, MTB smear is stained with carbol fuchsin based on its acid fastness, resistance of the bacilli to carbol fuchsin stain de-colorization. Upon examination under light microscope MTB appears as straight or slightly curved red rods.

In order to survive in harsh environmental conditions, the bacilli can build cell components directly from carbon and nitrogen sources (prototrophic), or use already synthesized carbon and nitrogen sources (heterotrophic) [33]. It is one of the slowest growing bacteria that have a generation time of 12 – 24 hours comparing with a 20 min doubling time for *E. coli*. The genome of mycobacterium is characterized with high guanine/cytosine (GC) content of about 70% and its cell walls possess high lipid content. Mycolic acid is the most abundant lipid content in the cell wall, contributing to TB immune resistance [33].

2. *Mycobacterium* underlying problems

2.1. *Mycobacterium* species

Mycobacterium genus includes a large diverse number of species (> 50) which can cause TB-like infection (non-tuberculous mycobacteria), or *Mycobacterium tuberculosis* complex (MTBC). These include: pathogenic, opportunistic, and non pathogenic human and animal infecting species [34, 35].

Non-tuberculous mycobacteria are classified into rapid and slow growing mycobacteria. Rapid growing mycobacteria give visible colonies in less than 7 days while slow growing mycobacteria give visible colonies up to 8 weeks incubation [35, 36]. They were first identified in the 1950s; however, their clinical concern emerged just in the last 2 decades with the rise of HIV epidemics [37]. These species are ubiquitous in different environmental sources such as soil, food, water, equipments, and aerosols. They can survive in a wide range of pHs, temperatures, and common

disinfectants [38, 39]. These characteristics permit nosocomial infections at high prevalence rates. Nevertheless, there is no evidence of non-tuberculous mycobacteria person-to-person transmission [35, 38]. Examples of these species are *Mycobacterium avium*, *M. intracellulare*, *M. abscessus*, *M. fortuitum*, *M. kansasii*, and *M. simiae*. Several research articles have reported pulmonary, skin and soft tissue infections, or disseminated diseases caused by non-tuberculous mycobacterium [35, 38, 40, 41].

MTBC consists of closely related species that cause TB infection to different hosts, these complex members are *M. tuberculosis*, *M. bovis*, *M. africanum*, *M. microti*, *M. caprae*, *M. canetti*, and *M. pinnipedii* [42, 43]. These members have DNA homology of about 85 – 100% [42]. MTB is the major cause of TB infection in humans. Animals can also get infected if contacted with infected humans [42]. *M. bovis* is the main cause of bovine TB which is due to the consumption of unpasteurized milk or dairy products. The established awareness campaigns against bovine TB have helped reducing incidence and prevalence rates in industrialized countries, where its prevalence is estimated as < 1% of all TB cases. It may increase in some populations [44]. *M. africanum* causes about 50% of pulmonary TB infections in Africa with higher estimates in HIV endemic populations [45]. *M. microti* is one of the rare mycobacterium species that was first described by Wells in 1937 from field voles, one of the most common mammals in Europe [46-48]. Caprine tuberculosis is caused by *Mycobacterium caprae* affecting goats, cattle, and cross infection to humans. It is predominant in Europe and causing a major health threat in Spain [49, 50]. *M. canetti* is a rare species that has been added to the *Mycobacterium tuberculosis* complex list recently. It was isolated from a farmer infected with pulmonary tuberculosis [42, 51]. Finally, *M. pinnipedii* has been isolated from seals and proved experimentally to infect guinea pigs and rabbits [52]. The transmission of *M. pinnipedii* to humans was documented in an outbreak of infection [53].

There are differences among non-tuberculous mycobacteria and MTBC with regard to transmission, infection, pathogenesis, and subsequently treatment. However, they have similar cell morphology and microscopic examination which is the most common method in developing countries, cannot be used to differentiate between them [35]. Therefore, it is crucial to differentiate between non-tuberculous mycobacteria and *Mycobacterium tuberculosis* complex members using discriminative molecular techniques.

2.2. Mycobacterium pathogenesis

The immune response plays a fundamental role in the defense against mycobacterium infection and pathogenesis. Basically, the immune response is divided into innate and adaptive immunity. Innate immune response is the natural immunity in which the immune cells face the pathogen for the first time but can eradicate it. However, adaptive immune response depends on previous pathogen contact information [54]. Tuberculosis is a latent infection in about 90% of cases without causing diseases while it is active in the remaining 10% of cases [33, 55-57]. It is proven that the transition from latent to active disease happens mainly when patients experience alteration in their immune system balance or became immunocompromised which is the reason behind the high prevalence of co-infection of HIV and TB (figure 5) [33, 55-57].

Tuberculosis infection starts with the inhalation of few mycobacterial cells that are released from an infected patient. The first cells to interact with the intruding mycobacterial cells are the alveolar macrophages and epithelial cells [55, 56]. The interaction of the bacilli with the alveolar macrophages takes place through different cellular macrophage receptors. The type of receptor determines the macrophage response. For instance, the interaction with Fc receptors increases the release of reactive oxygen intermediates that degrades the bacilli and permits the fusion of phagosomes with the lysosomes degrading the phagosomal content, where the bacteria reside. Thus macrophages could kill mycobacterial cells by both the oxygen and nitrogen radicals and lysosomal enzymes [55, 58]. After bacterial death, mycobacterial antigens are presented by class II major histo-compatibility complex members to CD4⁺ T lymphocytes [55]. This allows the production of interferon- γ (IFN- γ) and interleukin-12 (IL-12) leading to macrophage activation and more bacilli destruction [55]. CD4⁺ T lymphocytes also trigger apoptosis of the infected cells to decrease the number of bacterial viability and mediate CD8⁺ T cell response. CD8⁺ T cell mediated response acts mainly through cytokine production through secreting IFN- γ leading to bacterial destruction, and cytolytic function through lysing infected cells (figure 5) [55].

Nevertheless, the interaction of the bacilli with different surface receptors leads to different pathogenesis. For instance, bacilli interaction with macrophage complement receptor CR3 prevents the release of reactive oxygen intermediates (respiratory burst). Cholesterol assists in the mycobacterium and surface receptors

interaction. Upon engulfment of mycobacterium in phagocytosis, phagosomes maturation is arrested at early stage. Phagosomes-endosomes fusion is inhibited preventing bacilli destruction [55, 56, 58-60]. Blocking phagosomes maturation was found to be contributed by the retention of a protein called Tryptophane Aspartate Coat Protein (TACO) [55]. TACO protein prevents further maturation. Mycobacterial phagosomes are also characterized by interfering with phagosomal acidification and inhibit endosomal pathway fusion. The limited acidification is due to the low concentration of late endosome proton pump V-H⁺ ATPase. Phagosomal arrest is partial and some phagosomes develop to phagolysosomes (figure 6) [55, 56, 59, 60]. Mycobacterium bacilli secretes oxygen radical scavenger molecules such as lipoarabinomannan (LAM) and phenolic-glycolipid I [55].

Epithelial cells are also likely to be among the first cells to interact with mycobacterium since they are 30 times higher in number than alveolar macrophages. They can host and permit mycobacterium bacilli replication and are capable of triggering the release of IL-8 as a pro-inflammatory environment and nitric oxide [55]. Defensins, small endogenous antimicrobial cationic peptides which range in size from 30 – 50 amino acids, mediate another innate immunity response. These molecules can destroy microorganism's cell components and can pass through cytoplasmic membrane. Defensins show a promising treatment solution; however, their exact anti-mycobacterial mechanism is still unknown [55].

Since in the early infection stage T-helper 1 (Th1) mediated response such as IFN- γ and IL-2 showed a protective role against mycobacterium infection, late stage infection is characterized with down regulation of Th1 and activation of Th2 response. Late stages show elevated IL-4 levels, transforming growth factor (TGF- β) (which is produced by a specialized macrophage called foamy macrophage), high mycobacteria cells count, interstitial fibrosis, progressive pneumonia, and subsequent lung granuloma. This allows the shift from the production of pro-inflammatory to anti-inflammatory and immunosuppressive molecules from the early to the late stage, respectively. Granuloma is the immune-pathology hallmark of mycobacterium infection. It is composed of organized spherical structure of immune cells and bacteria, in which the core is bacteria, macrophages, and dendritic cells (DCs) surrounded by T- and B- lymphocytes. Figure 7 shows the different pathogenesis immune factors that are involved in tuberculosis infection [57, 59, 61].

2.3. Mycobacterium virulence and persistence factors

Virulence is a quantitative measure of pathogenicity [62]. *Mycobacterium tuberculosis* does not resemble other classical virulence factors such as toxins due to the complexity and occurrence of many factors involved in the infection. The most famous virulent factors are cell filtrate proteins ESAT-6 and HspX. Other virulence factors are categorized in table 1 [63].

All these virulence factors are related to exaggerating tuberculosis infection and persistence. These proteins, enzymes, and lipids are excellent molecular markers for diagnosis and already some of them are being used as antigens in vaccine development trials; however, more research is needed to confirm virulence role in infection and specificity of virulence factors to pathogenic MTB infection.

3. Current *Mycobacterium tuberculosis* diagnosis methods

Conventionally, TB diagnosis is based on Ziehl-Neelsen sputum staining using acid fast stain that is based on the ability of mycobacterium to resist acid de-colorization for its high mycolic acid content in the cell membrane (figure 4). However, this method cannot detect species and differentiate between tuberculous and non-tuberculous mycobacterium. It can detect TB within 5 min for each specimen but has a very low sensitivity (30 – 35% positive cases). It also could not detect recent infections since it depends on visual microscopic examination. The detection depends on finding at least 1 bacillus on the microscopic slide. However, it is still the current frontline diagnosis method in developing countries in particular governmental laboratories. Culturing on selective media that allows only TB to grow is also challenging as it is one of the slowest growing bacteria that needs at least 21 days to grow. Therefore, diagnostic tests based on emerging technologies are currently being developed to bypass these diagnostic challenges [14].

3.1. Culture methods

Culturing mycobacteria is considered as one of the less costly detection methods especially in screening purposes or in endemic countries. Solid and liquid medias are regarded as the gold standard for culturing mycobacterium; it takes from 3 to 8 weeks [4].

A new approach called “BACTEC 460”, Becton Dickinson Instrument Systems (Franklin Lakes, US) utilized a modified Middlebrook 7H12 automated detection system. $^{14}\text{CO}_2$ is detected after mycobacterium metabolizes ^{14}C radio-

actively labeled palmitic acid [15]. The main disadvantage of this method is the disposal of the radioactive waste (half life of ^{14}C is 5730 years). It detects mycobacterium within 5 – 10 days. This method is also expensive and cannot differentiate between different mycobacterium species [4, 14-16]. Another diagnostic approach is the integration of Accuprobe (Gen-Probe, US) with BACTEC to improve the BACTEC efficacy. It identifies series of *M. tuberculosis* complex, *M. avium* complex, *M. avium*, *M. kansasii*, and *M. gordonae*. The Accuprobe utilizes acridinium ester labeled ssDNA complementary to rRNA to detect various mycobacterium species. This detection method uses BACTEC culture for inoculation of suspected samples with subsequent sonication and addition of Accuprobe to form stable DNA:RNA hybrids followed by signal detection using a luminometer. Although Accuprobe can detect mycobacterium within 2 h; the needed for expensive devices such as a luminometer and a sonicator may represent a difficulty in large scale implementation especially in developing countries [17].

An integrated BACTEC and MGIT 960 (Becton Dickinson, Franklin Lakes, US) system can test 960 samples at the same time. It has a fluorometric sensor to detect oxygen utilization within 8 – 15 days [14, 17, 64]. In addition, Septi-check AFB biphasic media BBL (Roche) was also introduced in which the samples are aseptically transferred to the septi-check AFB bottle that contains high CO_2 Middlebrook content media and other supplements. Septi-check AFB slide of Middlebrook, egg-based media, and chocolate agar is incorporated, incubated, and inverted on a regular basis. Average number of days of detection ranges from 21 to 28 days [14, 65]. Another culture-based method, ESP II, is a non radioactive fully automated method (BD Difco, Franklin Lakes, USA). It monitors continuous pressure change from organism respiration. This system must be combined with other solid medium system to detect mycobacterium from 10 – 15 days [14].

3.2. Chromatography

This is based on detecting mycolic acid, the main cell wall component, unique peaks pattern using high performance liquid chromatography (HPLC) that could differentiate between different species. The method depends on the mycolic acid fingerprints library which was constructed based on species dependant mycolic acid derivatives [14, 66]. The main limitation of this method is that it requires the availability of HPLC in developing countries diagnostic laboratories, also it is saving

time consuming method for detection. It requires culturing, extraction, derivatization, and HPLC analysis [14, 66].

3.3. Bacteriophage based method

There are two approaches in bacteriophage based techniques; the first is based on infecting mycobacterium with phage D29, specific for mycobacterium, that will lead to insertion and subsequent amplification of phage genome in the target cells followed by progeny detection [14, 16, 17, 67]. If plaques form then the sample is determined to be positive for mycobacterium. Another approach is using luciferase reporter phages (LRP) allowing for luciferase enzyme transcription inside the target cells to detect the light produced if the sample is positive for TB when luciferin substrate is added [14, 16, 17, 67]. Bacteriophage D29 can be used to detect mycobacterium resistance depending on the ability to support phage infection in a medium containing rifampicin and isoniazid. Commercially available kits for those methods include FASTPlaque-TB® or PhageTek MB® for Biotec Laboratories Ltd, UK showing sensitivity of 70.3 – 75.2% and specificity of 98 – 99% [14, 17, 68]. FASTPlaque-MDRi which is also known as FASTPlaque-TB RIF™ detects indirectly rifampicin susceptibility. The test requires culturing of specimens on FASTPlaque rifampicin containing media. It depends on the growth of rifampicin resistant mycobacterium [69]. The assay is inexpensive, with detection time from 1 – 2 days. Although the assay can detect viable mycobacterial cells it cannot detect resistance other than rifampicin or mycobacterium complex species that directly affects selection of therapeutic regimens.

3.4. Immuno diagnostics

To improve the sensitivity of TB detection methods, immunologic based assays have been developed. The potential targets for immunologic diagnostics are either through specific antigen, antibody, or protein detection. However, some reported TB cases are suffering from delayed hypersensitivity that correspondingly will affect antibody detection giving false negative results [14].

There are various antigens specific for mycobacteria that can be detected by enzyme linked immunosorbent assay (ELISA), indirect ELISA (iELISA), reverse passive haemagglutinin test, and latex agglutination test. First, enzyme linked immunosorbent assay is a quantitative sandwich technique in which the antigen is detected using specific monoclonal antibody, mAb, and then the detection signal is indicated with a labeled secondary antibody specific for the antigen bound mAb. Its sensitivity reach up to 90% which is higher than 70.3 – 75.2% sensitivity of phage method; however, antigen cross reactivity may occur when the antibody developed is not highly specific. Also, ELISA is not an easy experiment that can be done on a regular laboratory work in developing countries. Indirect ELISA is the same idea but with antigen immobilized to detect a specific antibody [14]. The most commonly used antigens are glycolipids, lipopolysaccharides, lipoarabinomannan, antigen 5 (38 KDa), Esat-6 [70] and antigen 60 [14].

3.5. Molecular techniques

DNA based detection methods involve three different types: amplification, electrophoresis, and hybridization-based techniques. Table 2 summarizes molecular commercial techniques.

3.5.1. Amplification

3.5.1.1. Target amplification

Polymerase chain reaction (PCR) offers a rapid way to detect mycobacterium; it depends on selective primers design that bind to the flanking region of the target sequence, amplifies the sequence, and then visualizing the amplified bands using UV-light after gel electrophoresis and ethidium bromide staining or any other detection methods. Commercially, there is FDA approved Cobas® Amplicor (Roche Diagnostic Systems), that amplify 16s rRNA gene region in mycobacterium then the biotinylated amplicon hybridizes with immobilized oligonucleotide on micro titer plate. The sensitivity range was from 91 – 100% and detection is achieved within 6.5 h [17-19]. Advantages of PCR includes detection within about 24 h including sample processing but it is still expensive and requires highly trained technicians [14].

Transcription mediated amplification (TMA) is another PCR based method but amplifies rRNA isothermally using the advantage that rRNA targeting shows higher specificity. Gen-Probe® AMPLIFIED™ (AMTB) is a FDA approved commercial kit

that amplifies specific rRNA by DNA transcription then detection is based on hybridization probe assay, Gen-probe HPA, using ssDNA (single stranded DNA) probe chemiluminescent labeled. When RNA – DNA hybrid is formed they are detected with luminometer. The test lasts for 3.5 h but with 86.8% sensitivity and with no control [14, 17, 19].

Nucleic acid sequence based amplification (NASBA; Hain Lifescience, Germany) is considered as one of the TMA types. The method depends on having multiple copies of RNA from double stranded DNA (dsDNA) upon the action of T7 RNA polymerase [71]. Commercially, an integrated NASBA-DNA strip is done through magnetic bead capturing isolation and NASBA amplification of 23S rRNA followed by automated reverse hybridization. The assay is reliable and rapid, with specificity and sensitivity of 100% and 92%, respectively [17].

3.5.1.2. Probe amplification

Probe amplification method such as ligase chain reaction (LCR) is an assay that ligates 2 primers designed for detection after hybridization with the target, it depends on the presence of DNA ligase enzyme and nucleotides in the reaction. LCx MTB Abbot is used to detect mycobacterium within 6 hours with sensitivity and specificity of 74% and 98%, respectively. The main drawbacks are the need for trained personnel and high cost which limit its wide application [14, 71-74].

A semi-quantitative isothermal amplification via strand displacement amplification (SDA) is also developed. The method implies primer/probe amplification technique rather than target amplification based in which an initial target denaturation took place then each of the primer and the probe bind on the complementary target strand close to each other. The probe designed to have a restriction endonuclease site. First stage, DNA polymerase deficient exo-nuclease activity polymerizes by adding nucleotides extending the primer; 2' deoxyadenosine 5'-O-(1-thiotriphosphate), dATPaS, a modified nucleotide, is added in the reaction to be incorporated displacing probes.

Displaced probes bind to complementary primers allowing their extension with DNA polymerase. Second stage, the newly synthesized DNA : probe digested with restriction endonuclease enzyme; only the probe strand will be cut because of the incorporated dATPaS resulting in a nick formation which is extended by DNA polymerase again at the 3' end of the nick displacing the downstream strand. The

process continues for further exponential amplification process. Amplified segments can be detected using chemiluminescence hybridization system or integrated into any detection system. DProbe Tec ET assay utilizes a detection system based on fluorescence energy transfer. The method offers a sample free contamination system as the reaction is done in a single tube within 4 h; it has not been approved by FDA yet [14, 17, 19, 71].

3.5.1.3. Signal amplification

Amplification of the signal is done through a dual function probe that detects the target sequence and a branched amplifier. This system shows high sensitivity and detection signal. However, it is not available commercially [14].

3.5.2. Electrophoresis based methods

Restriction fragment length polymorphism (RFLP) is mainly used to detect mutations abolishing or creating restriction sites. Mycobacterium RFLP was used to detect mycobacterium species of amplified gene encoding heat shock protein. The test is reliable, cost effective, and results are ready within a day [75, 76].

Single stranded conformational polymorphism (SSCP) is employed to detect resistant mycobacterium having SNPs affecting ssDNA conformation. Resistant MTB ssDNA exhibits slightly different motility on polyacrylamide gel electrophoresis that can be distinguished from that of the reference strain [77].

3.5.3. Hybridization based methods

3.5.3.1. Line probe technology

This is based on amplifying specific sequences with biotinylated primers followed by reverse hybridization with immobilized probes in a parallel way on a simple strip having the advantage of banding pattern based colorimetric detection with an automated system with turnaround time within about 5 h. Two systems have been developed based on such technology: Inno Lipa Mycobacteria v2 (Innogenetics, Belgium) and Genotype mycobacterium (Hain LifeScience, Germany) [17, 19].

Inno Lipa Mycobacteria v2 is a strip test that identifies the most frequent 17 mycobacterium strains clinically isolated based on differences in 16s and 23s rRNA gene. The test showed 100% for both specificity and sensitivity with cross reaction between 2 rare mycobacterium species [17, 19]. Genotype mycobacterium is another assay available as two commercial kits: Genotype MTBC identifies *Mycobacterium tuberculosis* complex members based on gyrB gene polymorphism and Genotype mycobacterium CM for common species of mycobacterium based on 23S rDNA variations. Genotype MTBC failed to identify 3 species, *Mycobacterium tuberculosis* is one of them, due to typical hybridization pattern observed; all of them are easy to perform in standard laboratories. Sensitivity and specificity compared to sequencing for Genotype CM is 92.4% [17, 19].

3.5.3.2. DNA chips hybridization

DNA microarray is a hybridization technique using fluorescent labeled amplicons; detection is based on hybridization pattern and signal intensity. This method permits detection of large number of samples at the same time within 2 h; it is an expensive method [17]. CombiChip Mycobacteria (Geneln, Pusan, South Korea) used probes for 16s rRNA gene to differentiate between species [78].

3.6. Sequencing

Sequencing is the gold standard method in diagnosis either with sequencing directly or initial PCR followed with amplicon sequencing with automated sequencer [17]. Sequencing methods include manual sequencing of Maxam-Gilbert chemical sequencing, Sanger sequencing, and Pyrosequencing. The later technique detects pyrophosphate P_{Pi} release upon step by step nucleic acid synthesis [17]. Nonetheless, sequencing is not an economic choice for routine diagnosis. The most common target gene for sequencing is 16s rRNA because this gene encodes for both highly conserved sequences for genus identification and different species identification [17].

The MicroSeq System (Applied Biosystems, CA) is a commercial PCR based sequencing of 16s rRNA gene which showed reliable results [79]. Pyrosequencing™ (Biotage, Uppsala, Sweden) targeted about 30 bp of a highly variable sequence region A of 16s rRNA gene to differentiate between mycobacterium species [79].

4. Recent *Mycobacterium tuberculosis* trends in diagnostic approaches

Loop mediated isothermal amplification (LAMP) was developed to detect members of the mycobacterium complex using IS6110 repetitive insertion gene as a target. The test showed 20 times more efficiency than the conventional IS6110 test [80].

A micro fluidic biosensor has been developed for environmental screening of TB. The culture based chip is based on differentiation of TB from other bacteria based on the lipophilic property of the TB using paraffin. Incubated mycobacteria samples preferred adherence to hydrophobic surfaces such as paraffin due to mycolic acid content. Selective culturing of mycobacterium allowed their detection microscopically. The test is still a prototype [81].

A novel multi-channel piezoelectric quartz crystal (MSPQC) sensor system was developed for detection of rapid growth of *Mycobacterium tuberculosis* using an automatic continuous monitoring system. The system used to detect TB based on measurements of NH₃ and CO₂, the volatile metabolic products generated during growth, diffusing into the KOH absorbing solution, resulting in the change of conductance of the absorbing solution detected by the MSPQC accurately [82].

A gene chip has been developed to detect mycobacterium using the membrane oligonucleotide array method [83].

A number of nano-diagnostic assays have been developed for detection of TB. In 2006, Baptista *et al.* developed gold nanoparticles modified with probe specific to mycobacterium RNA polymerase β subunit gene. The test detects *Mycobacterium tuberculosis* in clinical sputum samples but after initial PCR round. The test detected up to 0.75 μ g of total DNA in 2 h time [84]. In 2009, Soo *et al.* used gold nanoparticles probes modified with thiol to identify *Mycobacterium tuberculosis* complex. They used two probes that are specific to part in IS6110 and Rv3618 DNA for targeting *Mycobacterium tuberculosis* complex and *Mycobacterium tuberculosis*, respectively. The test showed 96.6% sensitivity and 98.9% specificity for detection of *Mycobacterium tuberculosis* complex and 94.7% sensitivity and 99.6% specificity for detection of *Mycobacterium tuberculosis*; 600 samples were tested. The assay offered simple, rapid, cost-effective and accurate detection but used 2 PCR rounds to detect the targets and 1 day turnover [85]. Liandris *et al.* used DNA-gold nanoparticles probes specific to mycobacterium 16s – 23s internal transcribed spacer (ITS). Test detection limit was 18.75 ng DNA with 2 days turnaround time without the need for

DNA amplification [86]. Costa *et al.* developed another gold nanoprobe based mycobacteria test to detect *Mycobacterium bovis*, *Mycobacterium tuberculosis*, and *Mycobacterium tuberculosis* complex. Probes were specific to amplified gyrB DNA fragment of mycobacteria [87].

In 2010, Gazouli *et al.* employed a different nanotechnology approach. They developed magnetic beads conjugated with streptavidin and genus specific probe and fluorescent semiconductor quantum dots (QDs) conjugated with streptavidin and species specific probe to detect TB unamplified DNA. The probes were designed to target 23s rRNA gene part and IS6110 transposase. The assay is based on a sandwich hybridization method and used DNA isolated from formalin fixed paraffin embedded tissues (FFPE), bronchoalveolar lavage, and feces. The detection limit was shown to be up to 12.5 ng TB DNA in the reaction [88]. Li *et al.* developed a membrane transfer-based colorimetric mycobacterial DNA detection using alkaline phosphatase modified gold nanoparticles. Test detection limit was 0.23 pmol/L for 16s rDNA PCR product [89].

5. Gold Nanoparticles

5.1. Historic Background

Gold nanoparticles were shown to be extracted in the 5th millennium B.C near Bulgaria and in 1200-1300 B.C in China and Egypt, extraction reached around 10 tons gold per year [90, 91]. They used gold colloid in manufacturing ruby class colored ceramics and the most famous example is the Lycurgus cup. Then in 1618, the first book on colloidal gold was published by Doctor Francisci Antonii. In this book, the author described how to use the curative power of the soluble gold to treat and diagnose many diseases which had been illustrated with practical cases [90]. In 1857, Michael Faraday gave the birth to nanotechnology by discovering the reason behind different colors of gold nanoparticles and the reversible color change upon mechanical compression by studying their optical properties [90-92]. In the 20th and 21st century, an enormous number of reviews, experimental articles, and books have been published describing various synthesis methods, different physical and chemical properties, and fascinating biological applications of gold nanoparticles [28, 90].

5.2. AuNPs structure

Gold nanoparticles have several types; the two main types are the spherical AuNPs and nanoshells. Spherical AuNPs sizes range from 0.8 to 250 nm (generally from 1 – 100 nm) and have a UV-visible absorption spectrum at the visible region from 400 - 700 nm [20, 23, 28, 30]. Nanoshells are composed of gold metal as a thin shell layer surrounding a dielectric core of an inert material such as silica. Varying in the core/shell thickness alters the physicochemical properties of the nanoshell [23, 93]. These nanoshells range in size from 10-300 nm [23, 28].

5.3. AuNPs synthesis and Bio-conjugation

5.3.1. Synthesis

Generally, there are 2 main approaches in synthesizing nanoparticles: top-down or bottom-up approach. Top-down strategy involves the use of bulk materials to generate smaller nanoparticles through physical methods (mechanical or photolithography); bottom-up approach starts with molecular component of the nanoparticles, allowing for nucleation and growth of nanoparticles to the desired size through chemical methods [94].

The most common approach is the bottom up strategy through chemical methods. This method involves dissolving metal salt in an appropriate solvent followed by metal reduction to its zero valence state. The critical problem is that these metallic atoms in solution tend to aggregate. This could be achieved through using capping agents. These capping agents function through coating the surface of NPs, blocking its growth beyond the required size, and stabilizing the colloid formed in the solvent used. AuNP shape and size control is achieved through cautious selection of reaction conditions: time, temperature, and selection of reducing and capping agents [30, 94, 95].

5.3.1.1. Citrate reduction method

Citrate reduction method was introduced in 1951 by Turkevitch and is considered as one of the famous and conventional AuNPs preparation methods. The concept behind this method is that Au^{III} in gold III derivatives (HAu^{III}Cl₄ or NaAu^{III}Cl₄) is reduced to Au⁰ using reducing agent trisodium citrate [90, 91, 96, 97]. This method is used up till now as it is advantageous in the ease of replacing citrate shell with other ligands allowing for better stabilization and size control [90, 91, 97].

5.3.1.2. Shiffrin – Brust method

Shiffrin – Brust method was introduced in 1993 by Giersig and Mulvaney, they introduced the possibility of stabilizing AuNPs using different chain length of alkanethiols through the strong gold – sulfur bond. The concept here is that $\text{HAu}^{\text{III}}\text{Cl}_4$ is reduced by sodium borohydride (NaBH_4) in an organic solvent (toluene) and in the presence of thiol capping ligand (dodecanethiol (DDT)), also tetraoctylammonium bromide (TOAB) is used as a phase – transfer reagent [90, 97, 98]. This method is advantageous if functionalizing AuNPs surface with thiol ligands is required. Thiolated ligands are specific to biomolecules such as oligonucleotides or peptides [90, 91, 97]. The method synthesizes hydrophobic or also called monolayer protected clusters (MPCs) AuNPs [97].

5.3.2. Bio-conjugation

Functionalization methods involve modification of AuNPs based on the application. Unmodified AuNPs can be used directly for label free colorimetric detection methods. AuNPs can be functionalized with varied biomolecules either directly to their surfaces through covalent bonds (Au-S) or indirectly (specific recognition such as Au-S-antigen antibody or Au-S-biotin avidin). This is achieved by using ligands containing a sulfur group (such as thiolate or disulfide). This method offers higher stability of ligands with AuNPs and can be used for detecting antigens, antibodies, DNA, carbohydrates, proteins, peptides, or any biomolecules of interest while withstanding harsh experimental conditions [28, 30, 99, 100].

5.4. Physicochemical properties

5.4.1. Absorbance properties

AuNPs behave as other metal nanoparticles when exposed to light due to their shared photophysical properties. Their specific scattered light behavior is responsible for their intense red color. The incident light has an electromagnetic oscillating field. When this electromagnetic field has a wavelength smaller than the particles diameter, the nanoparticles induces a collective dipolar oscillation in the free conduction band electrons around the metal nanoparticles surface [23, 27, 28]. At specific frequency, the oscillation amplitude gets to the maximum. This frequency is known as Surface Plasmon Resonance (SPR) (figure 8) [27, 29-31]. The SPR is the reason behind the enhanced optical scattering and absorbance properties in the visible frequency range

(400 – 700 nm) and this can be identified using a spectrophotometer. Gold and silver nanoparticles (noble metals) specifically have stronger SPR bands compared to non plasmonic nanoparticles. Additionally, the SPR band wavelength and intensity are affected by the metal type, nanoparticles shape and structure, particle size, and the surrounding medium dielectric constant. For instance, increasing the AuNPs size causes red shift in the SPR wavelength [27, 29]. Another closely related phenomenon is plasmon - plasmon interaction in which AuNPs colloid aggregate together changing their color from red to blue. AuNPs can be induced for aggregation using electrolytes such as salt. Accordingly, this phenomenon is used in biomolecule detection and molecular diagnosis [23, 30].

5.4.2. Scattering properties

Light scattering occurs when AuNPs emit photons as a result of electron oscillation. These emitted photons can be either at the same frequency of the incident light and in this case are called “Mie or Rayleigh scattering” or at shifted frequency and in this case are called Surface Enhanced Raman scattering” (SERS) (figure 9). This energy shift is a result of molecular motion [27, 31]. The scattering properties of AuNPs make them a powerful tool in cell imaging techniques instead of traditional fluorescent dyes. This is because AuNPs have higher fluorescence and a stable signal. AuNPs scattering optical properties are highly dependent on particle size, they potentiate with larger particle size. For instance, 80 nm AuNPs in size show light scattering 10^5 fold higher than other traditional fluorescent molecules [27, 31, 32].

5.5. Detection methods

5.5.1. Non functionalized AuNPs

This method involves the use of unmodified AuNPs based on the electrostatic adsorption between citrate coated AuNPs and ssDNA leading to AuNP stabilization preventing its induced aggregation. This stabilization results from the weaker force of repulsion between nitrogenous bases of ssDNA and negative citrate coat of gold nanoparticles than that of dsDNA and AuNPs. This is because ssDNA can uncoil sufficiently causing adsorption between AuNPs and the exposed nitrogenous bases of the uncoiled ssDNA while dsDNA has a stable double helix structure exposing a negatively charged phosphate backbone. In the presence of a DNA target and enough salt concentration, ssDNA will complement with its DNA target preventing the

stabilization of gold nanoparticles allowing for its salt induced aggregation and consequent color change from red to blue. This is considered as the simplest method of ligand functionalization and is used mainly in label free colorimetric detection methods for dsDNA (figure 10) [28, 30, 99, 101, 102].

5.5.2. Functionalized AuNPs

5.5.2.1. Non cross-linking

In non cross-linking functionalization, AuNPs are linked to ssDNA for detecting ssDNA targets in the presence of salt allowing for gold colloid aggregation [103]. Biomolecules are linked to gold nanoparticles either directly to its surface through covalent bonds (Au-S) or indirectly (specific recognition such as Au-S-antigen/antibody or Au-S-biotin/avidin). This is achieved by using ligand containing sulfur group (such as thiolate or disulfide) [28, 90]. This functionalization method offers a higher stability for ligands with AuNPs and can be used for detecting antigens, antibodies, DNA, carbohydrates, proteins, peptides, or any biomolecules of interest as it can withstand relatively harsh reaction conditions (figure 10) [28, 30, 99, 100].

5.5.2.2. Cross linking

Another functionalization approach had first been reported in 1996 by Mirkin *et al.* and Alivisatos *et al.*, is the cross-linking method. This method depends on cross linking gold nanoparticles with – DNA conjugates together in the presence of a target of interest leading to a visual AuNPs color change [104, 105]. In cross linking, two sets of AuNPs get functionalized with two different probes complementary to the two target ends of a ssDNA target in a design of either head-to-head or heat-to-tail [104]. Mirkin *et al.* developed a different approach using a DNA linker complementary to AuNPs conjugate probes allowing bio-conjugation of AuNPs with different probes at a time [105]. Table 3 shows various detection methods for detection of AuNPs.

CHAPTER 3: Materials and Methods

1. Mycobacteria strains

For reference strains, two mycobacterium reference strains of *Mycobacterium H37Ra* and *Mycobacterium smegmatis* were cultivated and refreshed on Lowenstein Jensen solid media. Reference strains were obtained from Misr University for Science and Technology (MUST), faculty of pharmacy, Microbiology department. Media were supplied and prepared according to the manufacturer's protocol (Oxoid Ltd, Cambridge, UK) [106]. Middlebrook 7H9 broth media supplemented with Tween 80 and glycerol were obtained from BD Difco/ BBL (Becton, Dickinson and Company, Franklin Lakes, USA) [107].

For clinical strains, 11 anonymous clinical DNA samples isolated from TB patients were obtained from Misr University for Science and Technology (MUST), faculty of pharmacy, Microbiology department. An additional 14 clinical DNA samples isolated from TB patients were obtained from the U.S. Naval Medical Research Unit No.3 (NAMRU-3) (table 4).

2. Mycobacterial strains processing

2.1. Sample treatment

All mycobacteria samples were processed for DNA extraction according to established methods [108].

For reference strains, Cells were harvested from liquid media by centrifugation of each 250 mL aliquot at 2500 x g for 15 min at room temperature (Sigma Aldrich, Germany). Culture supernatant was decanted and cell pellets collected. Each cell pellet was re-suspended in 25 mL Tris-EDTA buffer (TE) (Promega, Wisconsin, USA) pH 8.0 and cells were centrifuged and harvested. All cell pellets were stored at -20 °C for a minimum of 4 h. This resulted in weakening of cell envelop and more efficient cell lysis [108].

2.2. DNA Extraction

For reference strains, Cell pellets were thawed and suspended in 5 mL TE buffer pH 8.0. An equal volume (5 mL) of chloroform / methanol (C/M) 2: 1 (Promega) were added and mixed for 5 min. This allowed for more efficient cell lysis as it removes most of the cell wall lipids. The suspension was centrifuged at 2,500 x g for 20 min at

room temperature. The mycobacteria formed a firm band at the organic-aqueous interface. So, tightly bacterial band was left in the tube and both the organic and aqueous layers were decanted. To remove the remaining of the organic solvent, the uncapped tube containing the depilated cells were put in water bath at 55 °C for 10 – 15 min. 5 mL of TE buffer pH 8.0 were added and the cells were suspended by vigorous vortex. 0.5 mL of 1M Tris-HCl (0.1 of the final volume) pH 9.0 was added to increase the pH of the cell suspension. 55 µL Lysozyme (10 mg/µL) (Promega) added to a final concentration of 100 µg/mL and incubated at 37 °C for 12-16 h. To remove cell proteins and contaminants, 0.5 mL 10% SDS (Promega) (0.1 volume of the final volume) and 60 µL of proteinase K (0.01 volume of the final volume) (Promega) were added. The extract was mixed by inverting the tubes up and down several times and incubated at 55 °C for 3 h.

Proteins were extracted from the resulting suspension by adding an equal volume of phenol / chloroform / isoamyl (P/C/I) 25:24:1 (Sigma Aldrich) and gentle shaking for 30 min followed by centrifugation at 12,000 x g for 30 min at room temperature. The aqueous layer was gently transferred to a sterile tube. To re- extract the aqueous layer, an equal volume of C/I 24:1 was added for 5 min with gentle rocking and repeat the step of centrifugation. The aqueous layer transferred again to a sterile tube. To precipitate TB genomic DNA, 0.1 of the total volume of 3 M sodium acetate (Sigma), pH 5.2, and 1 of the total volume of isopropanol (Sigma) were added. Tubes were inverted slowly to mix and stored at 4 °C for 1 h. The solution was centrifuged at 12,000 x g for 30 min at room temperature to pellet the DNA. The supernatant was discarded and the pellet washed with cold 70% ethanol. The DNA pellet re-suspended in nuclease-free water [108]. For digestion of isolated DNA, the DNA obtained was digested with a restriction enzyme *Bam* HI (Promega) according to the manufacturer's instruction by incubation at 37 °C for 1 hour followed by deactivation at 65 °C for 15 min. Five units *Bam* HI were required for each 1µg/µL DNA.

2.3. DNA quantification

DNA was diluted and absorbance measured at 260 and 280 nm using a double beam spectrophotometer (Shimadzu, UV-3600, Kyoto, Japan). DNA concentration was calculated using the formula:

$$\text{DNA Concentration } (\mu\text{g/mL}) = (A_{260})(50 \mu\text{g/mL})(\text{dilution factor})$$

3. Amplification of 16s rDNA gene segment

3.1. Primers design and analysis

Genomic sequences of *Mycobacterium H37Ra* and *Mycobacterium smegmatis* were obtained from NCBI genome database with (Gene Bank accession numbers: [CP000611](#) and [CP000480](#), respectively). PCR primers were designed using Invitrogen Vector NTI advance software using the obtained genomic sequences. For analysis, primers selected were investigated to avoid primer dimers, hairpin loops, palindromes, repeats, and assess their specificity for 16s rDNA. Primers were synthesized by Sigma (BIONEER, California, USA).

3.2. PCR

PCR was done using PCR master mix (Promega) and *Bam* HI digested DNA. BamHI restriction enzyme was selected based on the absence of a restriction site within the specified region. 5% Dimethyl sulfoxide (DMSO, Promega) was added in the master mix. DMSO was added to facilitate strand separation as it disrupts strong base pairing [109] due to the high GC content of mycobacterium [33]. For 50 μ L PCR reaction, 25 μ L PCR Master Mix 2X were added. 2.5 μ L of 10 μ M of each forward and reverse primer were added. 5 μ L of DNA template and 15 μ L nuclease-free water were added. PCR was done in 30 cycles: initial denaturation at 95 °C for 2 min, denaturation at 95 °C for 30 s, annealing temperature at 46 °C for 1 min, extension at 72 °C for 45 s, and final extension at 72 °C for 2 min in a thermal cycler (MyCycler, Bio-Rad, California, USA).

3.3. Semi nested PCR

Semi-nested PCR was done on purified amplicons. Genus and species semi-nested PCR were done in two separate reactions for each sample. Genus semi-nested PCR was done using the forward PCR primer and genus oligo-targeter as the reverse primer. In species semi-nested PCR, species oligo-targeter was used as the forward primer with the PCR reverse primer. This was done with master mix 2X (Promega) without the need for restriction digestion using PCR amplicons obtained previously as a DNA target. For 25 μ L PCR reaction, 12.5 μ L PCR Master Mix 2X were added. 1.5 μ L of 10 μ M of each forward and reverse primer were added. 5 μ L of DNA template and 4.5 μ L nuclease-free water were added. Semi-nested PCR was done in 25 cycles: initial denaturation at 95 °C for 2 min, denaturation at 95 °C for 30 s, annealing

temperature at 50 °C for genus and 52 °C for species for 1 min, extension at 72 °C for 45 s, and final extension at 72 °C for 2 min in a thermal cycler (Bio-Rad). Melting temperature for primers was calculated using the formula:

$$T_m = 64.9\text{ }^{\circ}\text{C} + 41\text{ }^{\circ}\text{C} \times (\text{yG} + \text{zC} - 16.4) / N$$

Where N is the number of primer bases

3.4. PCR amplicons: Purification, visualization, and quantification

PCR products were purified using QIAGEN PCR clean up kit (Purified PCR was separated using gel electrophoresis (Biorad) on 0.7% agarose gel, semi-nested on 1% agarose gel (Promega), were stained with ethidium bromide (Promega) and visualized using UV light. Photos were taken, analyzed and quantified using LabImage 1D software (Kapelan Bio-Imaging Solutions, Leipzig, Germany).

Purified PCR amplicon was diluted and absorbance measured at 260 and 280 nm using a double beam spectrophotometer (Shimadzu).

4. Gold nanoparticles synthesis

Spherical gold colloid was prepared using citrate reduction method [110]. Briefly, an aqueous solution of hydrogen tetrachloroaurate (III) ($\text{HAuCl}_4 \cdot 3\text{H}_2\text{O}$) (1mM) (99.99% Sigma Aldrich, Germany) was brought to reflux and stirred followed by a quick addition of 1% trisodium citrate solution. Solution color changed from yellow to wine red. The solution was then refluxed for an additional 15 min and left to cool at room temperature. The resulted spherical gold nanoparticles were filtered using a 0.45 μm pore size acetate filter (Sigma), and transferred into a clean storage glass bottle. Gold colloid absorption peak was scanned by spectrophotometer in the range of 400 – 700 nm with a concentration of 14 nM.

5. TB nano-gold assay

5.1. Oligo-targeters selection

Hybridization oligo-targeters of genus and species were selected from previous literature based on a conserved 16s rDNA gene part and synthesized by BIONEER [111]. Oligo-targeters were analyzed for specificity using NCBI Blastn tools and Invitrogen Vector NTI advance 11 software (Life technologies, New York, USA).

5.2. Detection of TB PCR and genomic DNA

5.2.1. Detection of PCR product

TB hybridization was optimized using different concentrations of NaCl (Sigma), phosphate buffered saline pH 7.4 (Sigma), phosphate buffered saline 0.3M NaCl (Sigma), PCR hybridization buffer, and Tris – HCl (Sigma). Genus and species oligo-targeters were used in different concentration ratios: 1:1, 1:2, and 1:3. Also hybridization with species oligo-targeter only was done.

Detection of PCR product was done by adding 44 mM NaCl, 2.5 μ L 1M Tris – HCl, 0.02 μ M oligo-targeters and 5 μ L PCR product followed by denaturation at 95°C for 30 s and annealing at 48°C for 30 s. Then 30 μ L gold colloid 13nm \pm 2 was added. Absorption peak for positive and negative was scanned by spectrophotometer in the range of 400 – 700 nm.

5.2.2. Detection of genomic DNA

Detection of genomic DNA was studied with addition of DMSO 2 – 5% (Promega). Several physical methods for shearing DNA such as vortex of DNA, vortex with glass beads, and DNA extraction with SiO₂ were tested. Chemical (enzymatic) digestion of DNA was done with *Hind III* restriction enzyme (Promega).

Detection of digested DNA was done by adding 10 mM NaCl, 0.083 μ M oligo-targeters, and 1 μ L DNA sample digested (containing the specified RE buffer E; Promega) followed by denaturation at 95 °C for 3 min and annealing at 48 °C for 1 min then 15 μ L of gold nanoparticles was added.

Detection of genomic DNA of 25 clinical strains was done using genomic DNA digestion by *Bam* HI restriction endonuclease (Promega). The assay was done by adding 2.5 μ L Tris HCl, 44 mM NaCl (0.5 M), 1 μ L species oligo-targeter (1 μ M), 4 μ L digested genomic DNA, and 3.54 μ L H₂O. The mixture was denatured at 95 °C for 3 min and annealed at 46°C for 1 min, then 30 μ L AuNPs was added. Positive and negative samples were scanned with a spectrophotometer in the range of 400 – 700 nm.

5.3. Detection limit of TB nano-gold assay

Nano-gold assay was done as previously mentioned with different DNA concentrations. A two fold serial dilution was done for PCR products of *Mycobacterium H37Ra* as a reference strain and one clinical strain for a DNA range

from 14.1 ng to 0.44 ng. Dilutions were tested with nano-gold assay as described above.

A two fold serial dilution was done for digested genomic DNA of a clinical strain of *Mycobacterium tuberculosis* complex (range from 40 ng to 10 ng). Dilutions were tested with nano-gold assay as described above.

The difference of detection limit between PCR product and digested genomic DNA was analyzed by calculating their corresponding molar concentrations according to the following formula:

Molar concentration (Picomoles/ μ l) = DNA Concentration (μ g/ml) / [0.66 X DNA Size (bp)]

CHAPTER 4: Results

1. DNA extraction

DNA extracted from reference and clinical strains was visualized clearly on 0.7% agarose gel electrophoresis (figure 11) and absorbance measured at 260 and 280 nm showed high purity and concentration of DNA.

2. Amplification of 16s rDNA gene part

2.1. Primers design and analysis

Using Invitrogen Vector NTI advance software, the best primer pair was selected from a list of possible primers based on lowest melting difference between the two primers. Primers obtained that can amplify 16s rDNA gene part are TBF: ACATGCAAGTCGAACGGAAAGG and TBR: CCTCCTGATATCTGCGCATTCCAC (table 5). For analysis, forward primer (TBF) was found to be free of palindromes, repeats, and hairpin loops with dG value (dG value indicates the spontaneity of a reaction to occur, negative value indicates double stranded PCR product) - 38.6 Kcal/mol while it has 3 dimers with dG values of - 2.0, - 1.8, and - 0.4 Kcal/mol. Reverse primer (TBR) was found to be free of repeats and hairpin loops with 2 palindromes at bases 7 and 13, with dG value of - 41.7 Kcal/mol while it has 2 dimers with dG values of -8.8 and -2.1 Kcal/mol.

2.2. PCR

PCR for reference and 2 clinical strains resulted in 16s rDNA target amplification and clear bands were visualized on 0.7% agarose gel electrophoresis. Bands' molecular weight was calculated using Lab Image 1D software and found to be in a range from 650 – 790 bp (figure 12). Total amount of DNA from purified PCR products were found to be around 130 ng with no protein or RNA contamination.

PCR for DNA of 9 anonymous clinical strains resulted in 16s rDNA target amplification and clear bands were visualized on 0.7% agarose gel electrophoresis. Bands' molecular weight was calculated using Lab Image 1D software and found to be in a range from 709 - 736 bp as shown in figure 13.

2.3. Semi nested PCR

Semi-nested PCR for reference and 2 clinical strains resulted in genus and species specific regions amplification confirming genus and species oligo-targeters specificity, respectively. *Mycobacterium smegmatis* showed no band for species. Bands' molecular weight was calculated using Lab Image 1D software. Genus semi-nested PCR resulted in bands length range from 167 – 186 bp. Species semi-nested PCR resulted in bands length range from 173 – 199 bp (figure 14).

Semi-nested PCR for 9 anonymous clinical strains DNA resulted in genus and species specific regions amplification confirming that the strains belong to *Mycobacterium tuberculosis* complex. Bands' molecular weight was calculated using Lab Image 1D software. Genus semi-nested PCR resulted in bands length range from 145 – 221 bp. Species semi-nested PCR resulted in bands length range from 168 – 259 bp (figure 15).

3. Gold nanoparticles synthesis

Spherical gold colloid absorbance peak was found to be at 520 nm with a diameter of $13 \text{ nm} \pm 2$ (14 nM) (figure 16).

4. TB nano-gold assay

4.1. Oligo-targeters selection

Selected genus oligo-targeter GR: AAAGTGCTTGTTGCGCTGTT and species oligo-targeter SF: ACCACAAGACATGCATCCCG were used in semi nested PCR and AuNPs detection. Nucleotide Blast of both oligo-targeters showed 40 – 50 alignment score (table 6). Genus oligo-targeter (100 blast hits) showed 100% query coverage for all mycobacteria sequences (figure 17) while species oligo-targeter (274 blast hits) showed 100% query coverage for only *Mycobacterium tuberculosis* complex members (figure 18).

4.2. Detection of TB PCR and Genomic DNA

Two versions of the nano-gold assay were developed. The first assay detected mycobacterium genus from other bacteria. The second nano-gold method differentiated *M. tuberculosis* complex from mycobacterium genus. Both nano-gold prototypes detected TB DNA both as PCR amplicons and genomic DNA.

4.2.1. Detection of TB PCR amplicon

PCR amplicons did not hybridize to target in presence of NaCl in different concentrations (30 mM – 70 mM), phosphate buffered saline (PBS) and PBS with 0.3M NaCl. Hybridization occurred with PCR buffer and NaCl with Tris – HCl. Genus and species oligo-targeters used in concentration ratio 1:1 showed positive results for all TB strains (figure 19), 1:2 and 1:3 ratios differentiated in *Mycobacterium smegmatis* (violet) from other mycobacterium (blue) (figure 20 and figure 21, respectively). The use of species oligo-targeter only resulted in a negative result (red color) for *Mycobacterium smegmatis* and positive color (blue) for other *Mycobacterium tuberculosis* complex (figure 22). Also, other bacterial DNA such as *E. coli* and *Staphylococcus aureus* showed negative results. Absorption peak for negative was at 525 nm and for positive was shifted to 550 nm (figure 23).

4.2.2. Detection of genomic DNA

Addition of DMSO 2 – 5% did not show hybridization of target to oligo-targeters. Also shearing of DNA with all physical methods was not sufficient to anneal DNA with oligo-targeters. Chemical digestion of DNA with *Hind III* restriction enzyme showed positive results. The first version of the assay differentiated mycobacteria genus from other bacteria using genus and species oligo-targeters (figure 24). The second developed assay detected *M. tuberculosis* complex using species oligo-targeter only (figure 25).

Detection of *Bam* HI genomic digested DNA for 25 clinical strains showed all strains as positive while control and *Mycobacterium smegmatis* digested genomic DNA remained negative (figure 26 and figure 27). Absorption peak for negative was at 525nm and for positive was shifted to 610 nm (figure 28).

4.3. Detection limit of TB nanogold assay

Amplified DNA detection limit was done for *Mycobacterium H37Ra* and clinical strain D and calculated to be 1 ng (figure 29).

Genomic digested DNA detection limit was done for *Mycobacterium tuberculosis* complex clinical strain number 3 and calculated to be 40 ng (figure 30).

CHAPTER 5: Discussion

This is the first study to use unmodified AuNPs in diagnosing MTBC. The assay employs genus and species specific oligo-targeters sequence (each is 20 nucleotides) that recognizes TB 16s ribosomal DNA (rDNA) gene (table 6) [111]. 16s rDNA has a highly conserved sequence among mycobacteria genus along with hyper-variable regions that differentiate the species of the same genus [112]. These oligo-targeters were designed based on sequence analysis of various mycobacterium species [111].

To confirm oligo-targeters specificity, the two oligo-targeters were blasted on Blastn NCBI database. Genus oligo-targeter showed 100% similarity to blast hits (no gaps) with all mycobacterium genus (100 hits). Alignment E value was $5e-04$ (the lower the E value, or closer to zero, the more significant) (figure 17). Species oligo-targeter showed 100% similarity to blast hits (no gaps) with all *Mycobacterium tuberculosis* complex (274 hits). Alignment E value was $5e-04$ (figure 18).

Using Vector NTI software, the two oligo-targeters were aligned on *Mycobacterium smegmatis* and *Mycobacterium H37Ra* complete genome of about 4411 Kb. PCR primers were designed for the selected 16s rDNA gene part. The resulted primer pairs were analyzed using the same software to select the lowest melting temperature difference (table 5). Selected PCR primers were blasted on NCBI Blastn to confirm specificity to all mycobacterium strains. Primers showed 100% identity with all mycobacterium.

First, a TB nano-gold assay was developed to detect *Mycobacterium tuberculosis* complex after PCR amplification. This assay was modified and optimized to directly detect TB using digested genomic DNA thus eliminating the need for PCR and reducing time and cost needed for diagnosis. The nano-gold TB detection experimental part is of two versions. The first version of the nano-gold TB assay was developed to distinguish mycobacterium genus from other bacteria using spherical AuNPs. The second version was optimized to detect and distinguish *Mycobacterium tuberculosis* complex from mycobacterium genus. Both nano-gold assays detected TB from PCR amplicons and genomic DNA.

Unidentified mycobacterium specimens were detected first by semi-nested PCR before AuNPs detection. Genus and species semi-nested PCR used PCR amplicons as a target DNA and employed genus and species oligo-targeters as reverse

and forward primers, respectively. Another aim for semi-nested PCR was to prove the specificity of the selected oligo-targeters. To confirm that genus oligo-targeter is specific for mycobacterium genus and species oligo-targeter is specific for *M. tuberculosis* complex.

The two reference strains selected for detection were *Mycobacterium smegmatis* as a negative control and *Mycobacterium H37Ra* as a positive control. Both *M. smegmatis* and *M. H37Ra* belong to the genus mycobacterium but only *M. H37Ra* belongs to *M. tuberculosis* complex. *Mycobacterium H37Rv* was not selected as it is a pathogenic strain. Reference strains were processed for DNA extraction. The most critical step in DNA extraction is cell wall lysis. The reason behind this is that the complex structure of mycobacterial cell wall and its high lipid content (figure 3) [6, 33]. The addition of chloroform / methanol removed a considerable quantity of the cell wall lipids. However, more research is warranted to optimize TB DNA extraction via a simple and fast process.

Before PCR, restriction digestion was used to allow the primers to access their hybridization targets. Analysis of the restriction sites was done by Vector NTI advance 11 software. *Bam* HI restriction enzyme was selected to digest TB DNA based on the absence of a recognition site in the selected amplified region (16s rDNA). DMSO was added to facilitate TB DNA strand separation [109] which is relatively difficult due to the high GC content of mycobacterium DNA [33]. Following PCR, purification was done to remove PCR buffer and excess primers that could affect the assay. Only thirteen PCR cycles were sufficient to exponentially amplify specific 16s rDNA gene segment in a range from 650 – 790 bp (figure 12).

For the anonymous clinical samples, PCR was done after genomic *Bam* HI restriction digestion and addition of 5% DMSO. The exponential amplification of 16s rDNA gene segment resulted in clear amplified specific bands in a range from 709 - 736 bp (figure 13). The difference in bands length is attributed to sequence variation or mutations in 16s rDNA.

Genus and species semi-nested PCR was then done to verify that the selected oligo-targeters targets' are within the amplified region. Semi-nested PCR resulted in amplified genus and species specific bands in length range 167 – 186 bp and 173 – 199 bp, respectively. Species semi-nested PCR of *M. smegmatis* showed no band. Species amplicons were slightly larger in length confirming specificity (figure 14).

To verify that the unidentified 9 specimens belong to MTBC. Semi-nested PCR was done as described previously. Genus and species semi-nested PCR resulted in amplified specific genus and species specific bands in length range 145 – 221 bp and 168 – 259 bp, respectively (figure 15).

Gold nanoparticles were synthesized to be within a size range of 13 ± 2 nm (14 nM). Spherical AuNPs were synthesized using trisodium citrate as the reducing agent. Citrate reduction resulted in nanoparticles with a negative surface charge [110]. Synthesized particles showed an absorbance peak at 520 nm (figure 16). Double stranded DNA detection is based on ssDNA oligo-targeters electrostatic adsorption on AuNPs surface. TB DNA extracted from clinical samples was denatured and permitted to anneal with 16s rDNA specific genus and species oligo-targeters in a suitable hybridization buffer and spherical AuNPs were then added. In the absence of the DNA target, oligo-targeters remain free. Upon addition of AuNPs, oligo-targeters uncoil sufficiently and their nitrogenous bases get adsorbed on AuNPs negative surface. Repulsion arises between exposed negatively charged phosphate backbone of adsorbed oligo-targeters. This allows dispersion and stabilization of AuNPs preventing their electrolyte induced aggregation. In the presence of the DNA target, each ssDNA of oligo-targeter will be hybridized to its complementary DNA strand. Upon addition of AuNPs, AuNPs aggregation occurs due to the presence of salt in the hybridization buffer. Negatively surface charged AuNPs interact with salt cation causing their aggregation. Induced aggregation leads to a shift in AuNPs absorbance peak from 520 nm to about 600 nm concurrent with a visual color change from red to blue (figure 31) [102, 113].

The nano-gold assay is affected by five factors: oligo-targeter concentration and length, salt concentration, AuNPs concentration, shape and size, denaturation/annealing temperature, and the hybridization buffer [102]. These factors were optimized for detection of *Mycobacterium tuberculosis* complex. The constant parameters in this study were the oligo-targeters length and AuNPs shape and diameter.

The first version of nano-gold assay was developed to detect mycobacterium genus from other bacteria. First, the color change between a negative control and a positive sample was adjusted using different salt, oligo-targeter and AuNPs concentrations. A problem was encountered with the hybridization of PCR amplicons

with oligo-targeters due to the high GC content [33]. Different hybridization buffers were used such as NaCl at different concentrations, PBS or PBS containing 0.3M NaCl. Hybridization occurred also using PCR buffer, proving that Tris base buffering capacity was required for mycobacterium hybridization. As PCR buffer has high chloride content providing unclear AuNPs visual difference, NaCl with Tris – HCl was used for hybridization. Since our target DNA is double stranded DNA, genus and species oligo-targeters used in concentration ratio 1:1. This showed all TB strains as a positive (including *M. smegmatis*, *M. H37Ra*, and 2 mycobacterium clinical strains) differentiating mycobacterium genus from other bacteria, *E. coli* and *Staph. aureus*, (figure 19).

The second version of nano-gold assay was optimized to detect and distinguish *M. tuberculosis* complex from mycobacterium genus. During the previous reaction, *M. smegmatis* amplified DNA was hybridized only with the genus oligo-targeter. Only half of the NPs aggregated shifting the visually observed color to positive. To circumvent this difficulty, lower genus oligo-targeter and higher species oligo-targeter concentration ratios were used. Genus and species oligo-targeters were used in concentration ratios of 1:2 (figure 20) and 1:3. A ratio of 1:3 improved *M. smegmatis* color change from reddish violet to violet and *M. H37Ra* and mycobacterium clinical strains as clear blue (figure 21). Moreover, using of species oligo-targeter only resulted in discriminative visual color difference. The assay showed the control and *M. smegmatis* as a negative (red) and *M. H37Ra* and mycobacterium 2 clinical strains as positives (blue) (figure 22). Positive samples showed an absorbance peak shift from 525 nm in negative samples to 550 nm broad band (figure 23). This is the first time to report the use of a single oligo-targeter in unmodified AuNPs detection method for TB detection.

Previous literature explained that target DNA is denatured completely and the two complementary oligo-targeters hybridize with the two strands. This contradicts with the results because the use of a single oligo-targeter would allow the genus oligo-targeter to hybridize with one target strand leaving the other to stabilize the AuNPs. The possible explanation is that long (target) ssDNA do not stabilize AuNPs. Another probable explanation is that the target DNA denatures and/or anneals in a similar way to a replication bubble. Then each oligo-targeter of them anneal. This would allow one oligo-targeter to anneal with the target in the replication bubble with complete AuNPs aggregation (figure 32).

Detection limit for PCR products was about 1 ng DNA (figure 29) which is the lowest compared to other reported nanoparticles based mycobacterium diagnosis assays. Baptista *et al.* test detected up to 0.75 μg [84], Soo *et al.* detected 0.5 pmol of PCR product (about 40 ng) [85] and Liandris *et al.* employed the use of DNA - gold nanoparticles conjugates with a detection limit of 18.75 ng [86]. Finally, Li *et al.* developed a membrane transfer-based colorimetric mycobacterial DNA with a detection limit of 0.23 pmol/L [89].

To eliminate the need for PCR and save time in diagnosis, genomic DNA is used as a target for the previous optimized two nano-gold assays. As mycobacterium genomic DNA is GC rich, it was difficult to denature and hybridize. The addition of DMSO 2 – 5 % did not allow for hybridization but facilitated the aggregation of AuNPs. The promising solution was to shear mycobacterium DNA. Physical methods of shearing include: vortex, vortex with glass beads, and sucking DNA in a syringe needle. All these physical methods failed to shear mycobacterium genomic DNA. Another method of DNA extraction using silicon dioxide was proven to shear bacterial DNA [114]. The method was tried on both *E. coli* and mycobacterium DNA. It resulted in complete shearing of *E. coli* DNA while mycobacterium DNA did not shear. The other way of DNA shearing is chemical digestion via the use of restriction endonucleases. Restriction digestion of mycobacterium DNA with optimization of salt concentration allowed for oligo-targeter – target hybridization directly from genomic DNA (figure 24 and figure 25).

Detection of digested genomic DNA using AuNPs was done and resulted in a sharp positive color change for all 25 *Mycobacterium tuberculosis* clinical strains (figure 26 and figure 27). This result confirms that the assay detected *Mycobacterium tuberculosis* complex using unmodified AuNPs with a single oligo-targeter. A UV-visible absorbance peak of a negative sample was at 525 nm while for positive digested genomic DNA samples showed UV-visible absorbance broad peak shift to 610 nm (figure 28).

Detection limit for digested genomic DNA was 40 ng DNA (figure 30). The difference of detection limit between PCR product and digested genomic DNA is attributed to the higher copy number of target DNA in PCR amplicons than in genomic DNA. To proof that, the molar concentrations for both the PCR product and genomic DNA were calculated (table 7). Molar concentration of PCR product was

12440 pM while of genomic DNA was 3.49 pM. The wide variation between the molar concentrations of the PCR product and genomic DNA could explain the difference in detection limit. Another factor is the restriction digestion time, longer restriction time allows more oligo-targeters to hybridize to their DNA target.

CHAPTER 6: Conclusions and Future Prospects

Since the identification of *Mycobacterium tuberculosis* in 1882 by Robert Koch, TB diagnosis has been challenging. Airborne mode of transmission, lung persistence, lack of rapid, sensitive and cost effective identification as well as the declined efficacy of the solely existing vaccine, BCG, has encumbered MTBC detection. In this research, unmodified spherical AuNPs were used for direct detection *Mycobacterium tuberculosis* complex DNA after PCR amplification. A second version of the assay detected TB DNA directly after restriction digestion of TB genomic DNA isolated from clinical specimens using a single oligo-targeter that recognizes 16s rDNA gene segment. The assay detection limit was 1 ng for PCR product and 40 ng for digested genomic DNA. The assay showed 100% sensitivity and 100% specificity as compared with bacterial culture method (gold standard) and semi-nested PCR. The assay turnaround time is about 1 hour including sample digestion and detection of extracted DNA. The TB nano-gold assay is inexpensive and does not require sophisticated instruments or expensive reagents. Consequently, this assay is a promising candidate as a frontline test for diagnosing *Mycobacterium tuberculosis* complex. After optimization, it can replace the Ziehl-Neelsen staining detection method in developing countries.

Several developments of the developed prototype include further testing using non-tuberculous species to further confirm specificity such as *M. avium*, *M. intracellulare* and *M. abscessus*. A multi copy specific conserved TB DNA sequence will be targeted to improve the assay detection limit. Due to mycobacterium high lipid contained cell wall DNA extraction is a time consuming process (1-2 days). Thus, a second improvement will involve the development of rapid DNA extraction procedures to extract TB DNA directly from sputum samples. To avoid personal bias that may be encountered during visual detection of color change, a small reader will be produced that detects color change spectrophotometrically. Another version of the TB nano-gold assay will be developed and optimized for direct detection of MDR and XDR *Mycobacterium tuberculosis* strains using multi-oligotargeters.

CHAPTER 7: Tables

Table 1. Mycobacterium cell virulence factors exaggerating tuberculosis infection and persistence

Virulent factors	Types	Ref.
Cell secretion and envelope function	<ol style="list-style-type: none"> 1. Cell filtrate proteins such as ESAT -6, CFP-10 and HspX 2. Cell surface components such as LAM, Erp and Mas 	[63]
Enzymes involved in cellular metabolism	<ol style="list-style-type: none"> 1. Fatty acid and Lipid metabolism such as ICI 2. Amino acid synthesis genes such as LeuD 3. Oxidative stress proteins and anaerobic respiration such as KatG 	[63]
Transcription regulators	<ol style="list-style-type: none"> 1. Response regulator such as PhoP 2. Sigma factors such as Sigma A 	[63]

ESAT-6: Early secretory antigenic target (6kDa). CF-10: Culture filtrate protein. HspX: Heat shock protein. LAM: Lipoarabinomannan glycolipid. Erp: Surface located protein. Mas: Mycocerosic acid synthase. ICI: Isocitratelase enzyme. LeuD: Isopropylmalate Isomerase enzyme. KatG: catalase;peroxidase enzyme. PhoP: Phosphatase response regulator.

Table 2. Commercial molecular techniques for detection of *Mycobacterium tuberculosis*

Commercial technique	Detection method	Main advantage	Main disadvantage	Ref.
Cobas® Amplicor	PCR	Target: 16s rDNA Detects in 6.5 h Sensitivity 91 %	<ul style="list-style-type: none"> • Requires PCR • Trained personnel • Expensive • Depends on culturing 	[17-19]
Gen-Probe® AMPLIFIED™	TMA	Target: 16s rRNA Detects in 3.5 h Sensitivity 86.8 %	<ul style="list-style-type: none"> • Requires PCR & Luminometer • Trained personnel • Expensive • Depends on culturing 	[14, 19]
Inno Lipa Mycobacteria v2	Line probe hybridization	Target: 16-23s rDNA Detects in 5 h Sensitivity 100 %	<ul style="list-style-type: none"> • Requires PCR • Trained personnel • Expensive • Depends on culturing 	[17, 19]
Genotype MTBC	Line probe hybridization	Target: gyrB gene Detection time N/A Sensitivity N/A	<ul style="list-style-type: none"> • Failed to identify 3 species, including <i>M. tuberculosis</i> • Depends on culturing 	[17, 19]
MicroSeq System	Sequencing	Target: 16s rDNA Detection time N/A Sensitivity N/A	<ul style="list-style-type: none"> • Requires PCR • Requires sequencer • Trained personnel • Expensive • Depends on culturing 	[17]

PCR: polymerase chain reaction. TMA: transcription mediated amplification.

Table 3. Selected gold nanoparticles detection methods and their biological applications

Detection by	Detection method	Detection limit	Clinical biological targets	Clinical samples	Ref.
Colorimeter	Non cross-linking unmodified AuNPs	2 fmol – 100 fmol	Hepatitis C virus ^{a, b}	RNA, human plasma	[115, 116]
			SNPs ^a	genomic DNA, human whole blood	[117]
			SNPs associated with long QT syndrome KCNE1 gene	genomic DNA	[102]
Light scattering imaging	Cross-linking aggregation	33 zmol	Methicillin resistant <i>Staphylococcus aureus</i> and <i>S. epidermidis mecA</i> gene	DNA, cultured bacteria	[118]
Naked eye or UV visible spectroscopy	Non cross-linking aggregation	375 zmol	K-ras oncogene	genomic DNA, adenocarcinoma cell lines	[84]
		4.2 pmol	β- thalassemia mutations	genomic DNA, human blood	[119]
		100 nmol L ^{-1 a}	Mycobacterium tuberculosis	DNA, clinical specimens	[120]
Light scattering imaging	Sandwich hybridization	250 zmol – 10 amol	Coagulation genes	genomic DNA	[121]
			Gene expression in human brain	total brain RNA	[122]
			Methicillin resistant <i>Staphylococcus aureus mecA</i> gene	DNA, cultured bacteria	[123]

SNP: Single nucleotide polymorphism. KCNE1: Potassium voltage-gated channel subfamily E member 1.

^a May involve PCR

^b May involve RT-PCR

Table modified from [30].

Table 4. Mycobacterium strains used in this study

Mycobacterium strains	Number of samples	Strains analysis	
		Mycobacterium genus	<i>Mycobacterium tuberculosis</i> complex species
<i>Mycobacterium tuberculosis</i> clinical strains	14	+	+
Anonymous TB clinical strains	11	+	+
<i>Mycobacterium H37Ra</i>	1	+	+
<i>Mycobacterium smegmatis</i>	1	+	–
Other bacterial strains (<i>Staphylococcus aureus</i> and <i>E. coli</i>)	2	–	–

Table 5. PCR primers used for amplification of TB 16s rDNA

Genes	PCR primers sequences'	Tm at Vector NTI software (° C)	Length of PCR product (bp)	Genomic coordinates (bp)
16S rDNA	TBF: ACATGCAAGTCGAACGGAAAGG	51.5	<i>M. H37Ra:</i> 650 bp	<i>M. H37Ra:</i> (1473211-1473860)
	TBR: CCTCCTGATATCTGCGCATTCCAC	54.4	<i>M. smegmatis:</i> 638 bp	<i>M. smegmatis:</i> (3824449-3825086)

TBF: Mycobacterium forward primer

TBR: Mycobacterium reverse primer

Table 6. Selected mycobacterium 16s rDNA specific oligo-targeters

Oligonucleotide designed sequences	Blast hits	Alignment identity
TBG: TTGTCGCGTTGTTGCGTGAAA	100	100% for different mycobacteria species
TBS: ACCACAAGACATGCATCCCG	274	100% for mycobacteria strains from <i>M. tuberculosis</i> complex

TBG: Mycobacterium genus oligo-targeter

TBS: *Mycobacterium tuberculosis* complex species oligo-targeter

Table 7. Concentrations of PCR products and digested genomic DNA

	DNA length (Kb)	Concentration (ng/μL)	Molar Concentration (pM)	Detection Limit (ng)
PCR product	0.7	5.65	12440	1 ng
Genomic DNA	4411	10	3.49	40 ng

DNA Concentration (μ g/mL) = (A260)(50 μ g/mL)(dilution factor)

Molar concentration (Picomoles/ μ l) = DNA Concentration (μ g/ml) / [0.66 X DNA Size (bp)]

CHAPTER 8: Figures

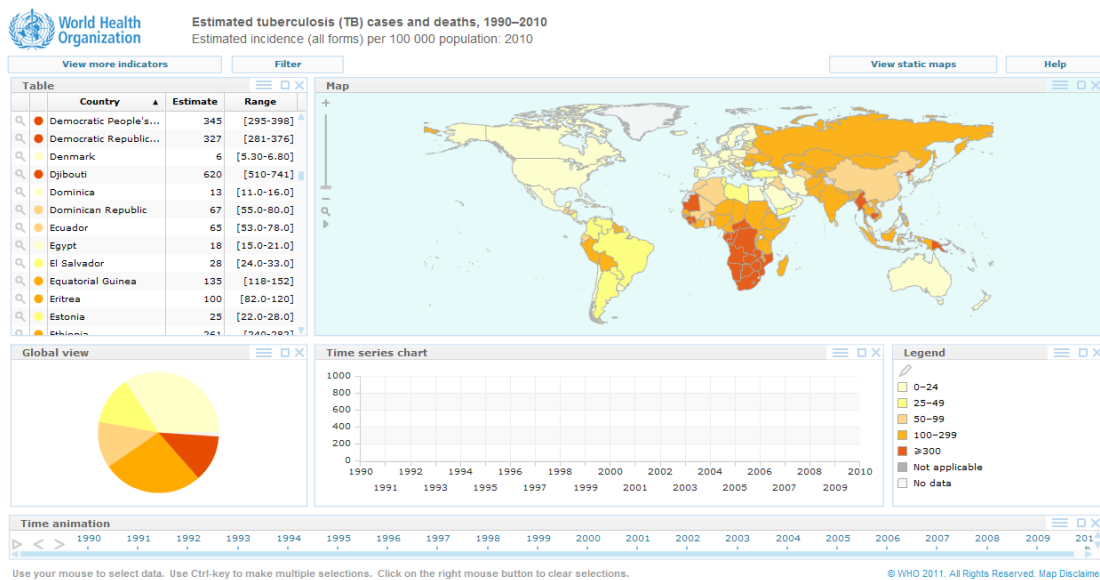


Figure 1. WHO Tuberculosis incidence estimates in 2010

The figure shows five discriminatory legend colors for different incidence ranges. The highest range is more than or equal to 300 per 100 000 population per year which is reported in South Africa. The lowest range is from 0 – 24 per 100 000 population per year which is observed in Egypt (18 per 100 000 population), Saudi Arabia (18 per 100 000 population), Canada (4.7 per 100 000 population), and United States (4.1 per 100 000 population). Figure reproduced from: http://gamapserv.who.int/gho/interactive_charts/tb/cases/atlas.html

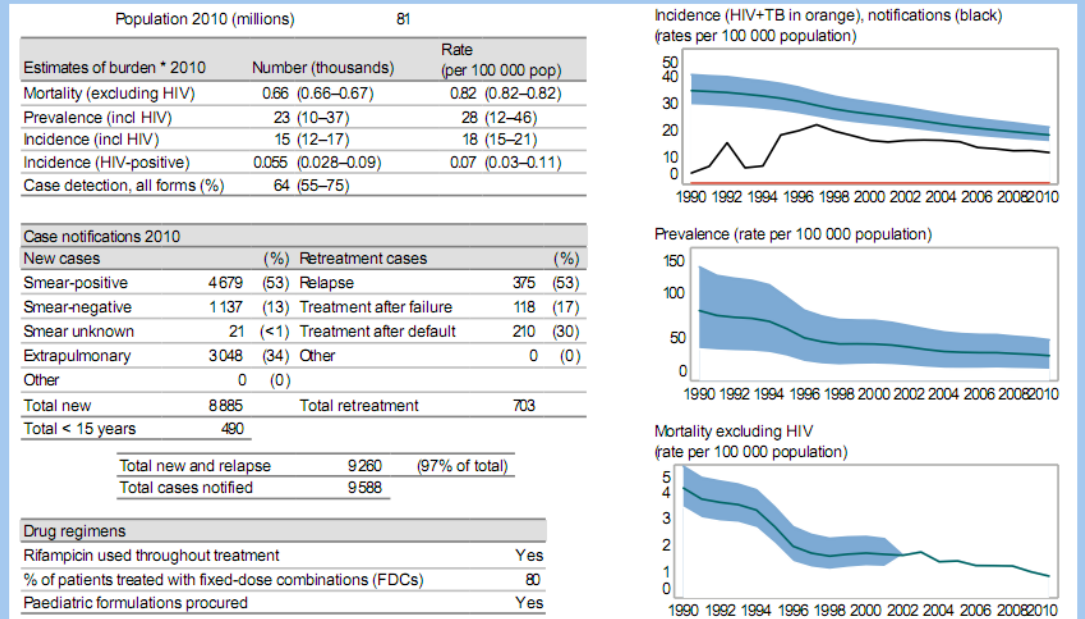


Figure 2. TB incidence, prevalence, and mortality rates in Egypt

Egypt TB estimated incidence rate was 18, prevalence rate was 28, and mortality rate was 0.82 per 100 000 population [2]. Figure reproduced from:

https://extranet.who.int/sree/Reports?op=Replet&name=%2FWHO_HQ_Reports%2FG2%2FPROD%2FEXT%2FTBCountryProfile&ISO2=EG&outtype=html

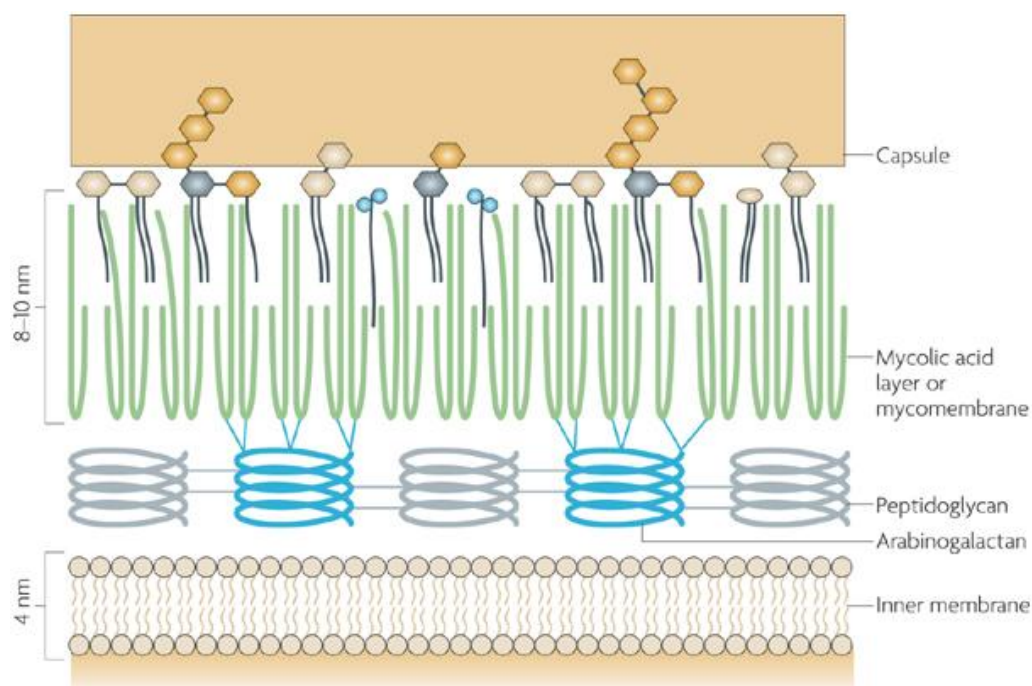


Figure 3. Schematic representation of mycobacterial cell wall

Mycobacterium cell wall is composed of three layers. The first is cytoplasmic membrane layer. Inner membrane is linked to the cell wall core layer. This stratum contains three different covalently linked structures: peptidoglycan (grey), arabinogalactan (blue) and mycolic acids (green). The peptidoglycan is attached to arabinogalactan via a disaccharide phosphate linker. The arabinogalactan is a branched-chain polysaccharide. The hexaarabinofuranosyl termini of arabinogalactan are linked to mycolic acids through ester bonds. The covalent linkage of mycolic acids results in a hydrophobic layer. Mycolic acid layer is also called mycomembrane. The outer part of the mycomembrane contains a variety of free lipids, such as phthiocerol dimycocerosates, phenolic glycolipids, dimycolytrehalose, sulpholipids and phosphatidylinositol mannosides. Most of these lipids are specific for mycobacteria. The outer-most layer, which is commonly called the capsule, mainly contains polysaccharides such as glucan and arabinomannan. Figure reproduced from [6].

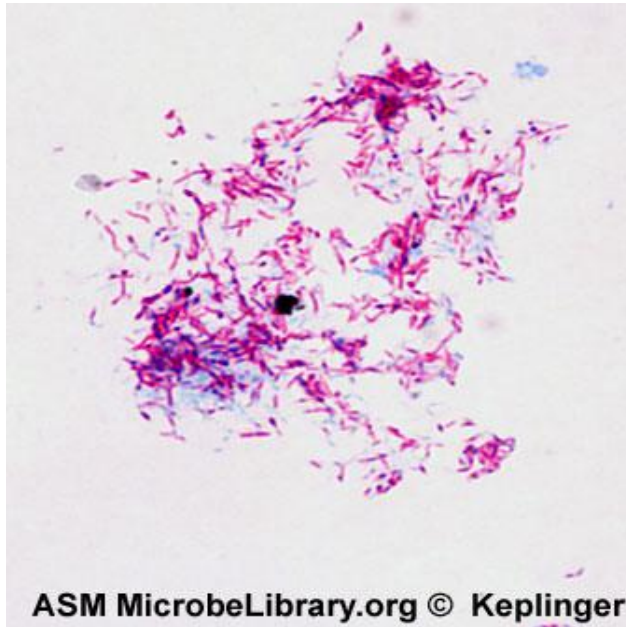


Figure 4. Acid fast stain of mycobacterium cells

Mycobacterium tuberculosis smear is stained with carbol fuchsin based on its acid fastness upon examination under light microscope; it appears as straight or slightly curved red rods. The staining requires floating of the suspected slide in carbol fuchsin stain with continues heat exposure for 5 min after stain boiling. De-colorization of slide using 1% acid alcohol. Counter staining occur with methylene blue for 30 s. Rinse with water and allowed for microscopic examination. The detection depends on detecting at least a bacillus in the microscopic slide. It is the current detection method used in developing countries. Figure reproduced from: http://www.microbelibrary.org/microbelibrary/files/ccImages/Articleimages/Atlas_AcidFast/Mycobacteriumsmegmatis_AcidFast_fig3.jpg

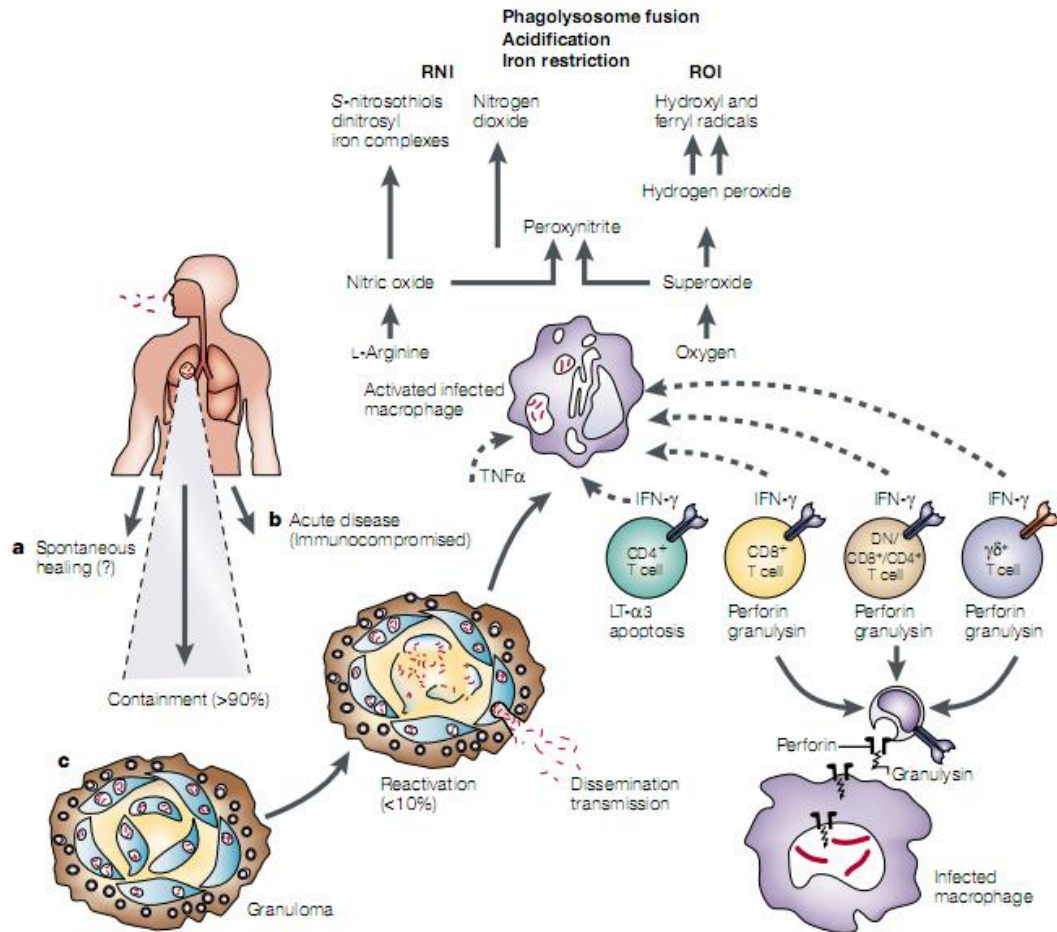


Figure 5. Mycobacterium tuberculosis infection: Three outcomes

Human infection of *Mycobacterium tuberculosis* has three main mechanisms. A) Spontaneous healing of infected human is postulated with a minute percentage. B) Direct development of an active disease infection usually occurs in immunocompromised patients. C) Containment of mycobacterium bacilli in about 90 % of patients resulting in latent infection. Latent infection develops into active disease upon reactivation. At the site of infection (granuloma), T cells and infected macrophages controls the infection with the production of interferon- γ and tumour necrosis factor- α . Activated infected macrophages allow the production of antimicrobial agents such as reactive nitrogen and oxygen intermediates. IFN- γ : Interferon- γ . TNF- α : Tumour necrosis factor- α . RNI: Reactive nitrogen intermediates. ROI: Reactive oxygen intermediates. Figure reproduced from [60].

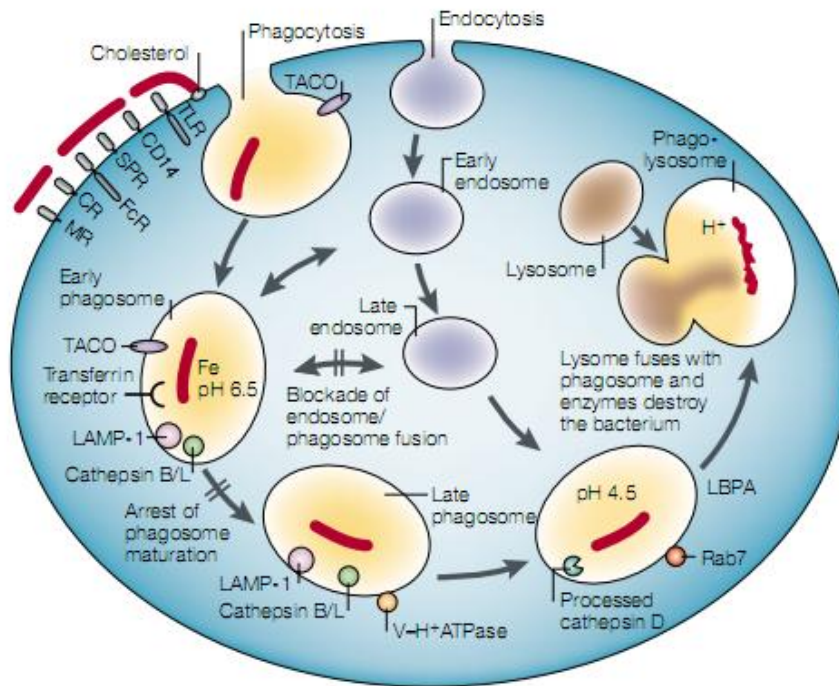


Figure 6. The intracellular pathogenesis of mycobacterium infection

The interaction of the bacilli with a variety of surface receptors leads to different pathogenesis. Cholesterol assists in the mycobacterium and surface receptors interaction. Upon engulfment of mycobacterium in phagocytosis, phagosomes maturation is arrested at early stage. Fusion of phagosomes with endosomes is inhibiting preventing bacilli destruction. Blocking phagosomes maturation was found to be contributed by the retention of TACO protein. TACO prevents further phagosomes maturation. Mycobacterial phagosomes interfere with phagosomal acidification and inhibit endosomal pathway fusion. The limited acidification is due to the low concentration of late endosome proton pump V-H⁺ ATPase. Phagosome arrest is partial and some phagosomes develop to phagolysosomes. MR: Mannose Receptor. CR: Complement Receptor. FcR: Receptor for the constant Fragment of immunoglobulin. SPR: Surfactant Protein Receptor. TLR: Toll-like receptor. TACO: tryptophane aspartate-containing coat protein. LAMP-1: Lysosomal-Associated Membrane Protein 1. V-H⁺ATPase: vacuolar ATP-dependent proton pump. Rab7: Member of the small GTPase family. LBPA: Lysobiphosphatic acid. Figure reproduced from [60].

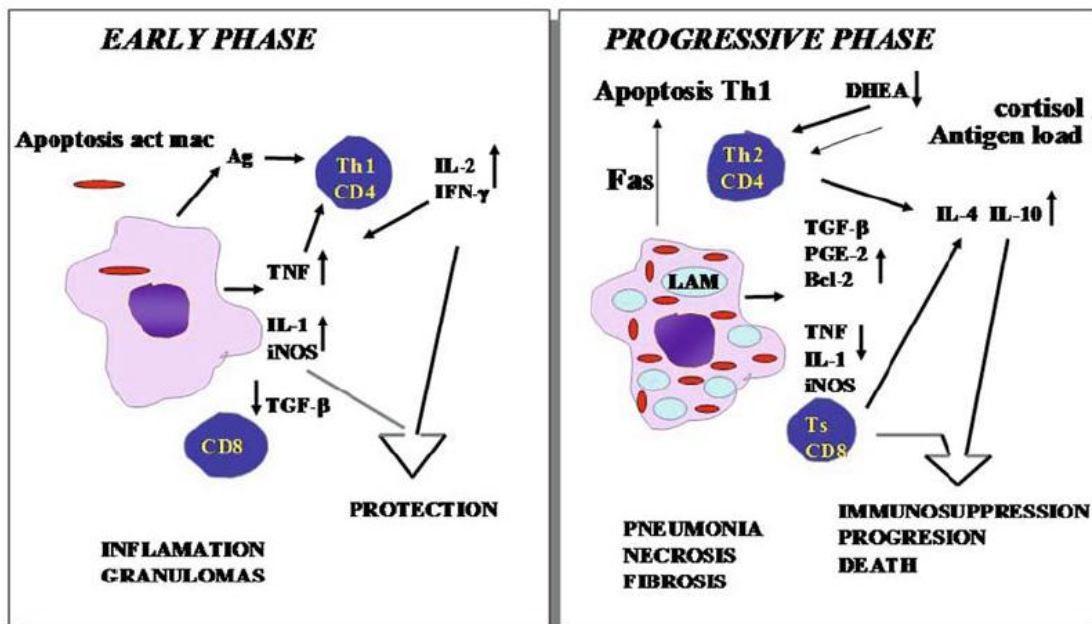


Figure 7. Immune factors affected by tuberculosis infection

Pathogenesis of mycobacterium causes shift from the production of pro-inflammatory to anti-inflammatory and immunosuppressive molecules. In the early infection stage, a protective role against mycobacterium infection showed T-helper 1 mediated response such as IFN- γ and IL-2. However, late infection stage is characterized with down regulation of Th1 and activation of Th2 response. Progressive infection stage shows elevated IL-4 levels and TGF- β leading to high mycobacteria cells count, interstitial fibrosis, progressive pneumonia, and subsequent lung granuloma. Figure reproduced from [55].

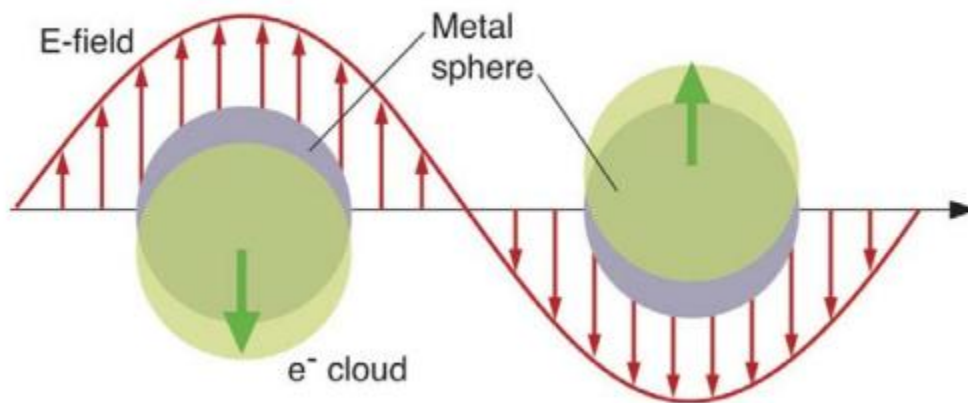


Figure 8. Surface Plasmon Resonance (SPR) of gold nanoparticles

When a light hits AuNPs, light has an electromagnetic field of a wavelength larger than AuNPs diameter, the nanoparticles induces a collective dipolar oscillation for the free conduction band electrons around the metal nanoparticles surface. At a specific frequency, the oscillation amplitude gets to a maximum. This frequency is known as Surface Plasmon Resonance band. Figure reproduced from [29].

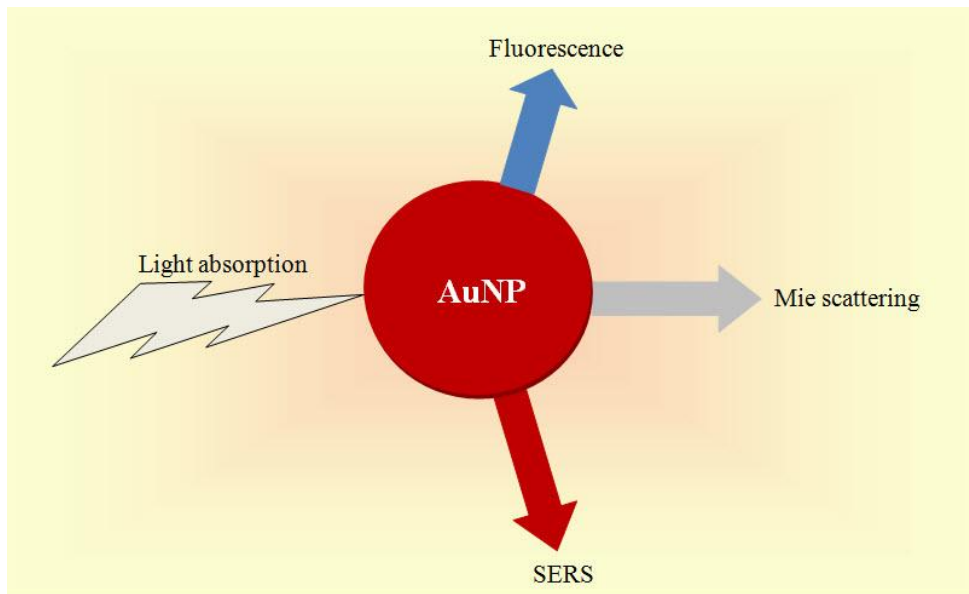


Figure 9. Optical properties of gold nanoparticles

Gold nanoparticles interaction with light resulted in absorption and scattering properties. As a result of electron oscillation, gold nanoparticles emit photons in the form of scattered light. These emitted photons can be either at the same frequency of the incident light and termed “Mie or Rayleigh scattering” or at a shifted frequency from the incident light and called “Surface Enhanced Raman scattering”. Figure modified from [31].

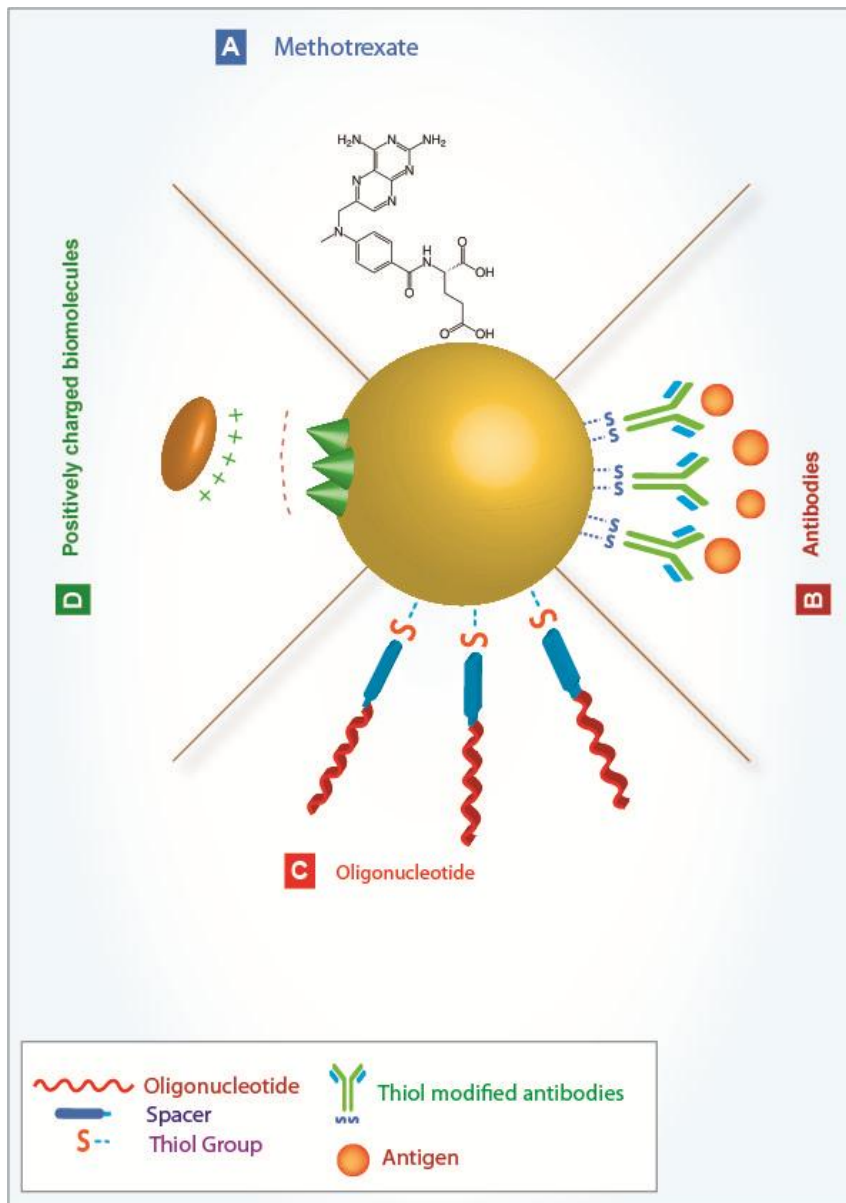


Figure 10. Different methods for functionalization of gold nanoparticles

Gold nanoparticles are functionalized in different techniques to varied biological biomolecules. A: Negatively charged biological molecules are adsorbed to gold nanoparticles directly to its surface. B: Biological molecules are linked indirectly through specific recognition such as Au-S-antigen antibody. C: Biological molecules are linked indirectly through specific recognition through Au-S-avidin biotin. D: Biological molecules are linked to gold nanoparticles through surface electrostatic adsorption.

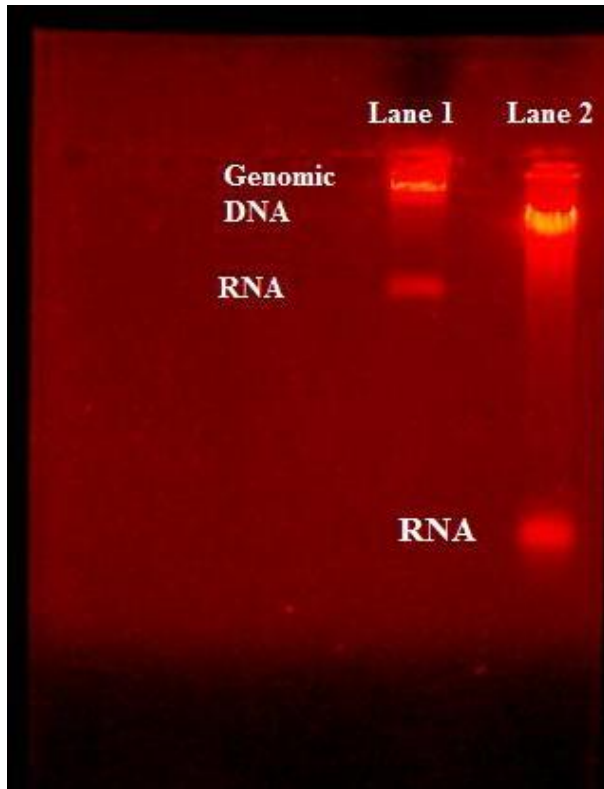


Figure 11. Agarose gel electrophoresis of extracted genomic mycobacterial DNA

Mycobacterium genomic DNA extracted was separated using gel electrophoresis on 1% agarose gel, stained with ethidium bromide, and visualized using UV light. Lane 1: *Mycobacterium smegmatis* genomic DNA. Lane 2: *Mycobacterium H37Ra* genomic DNA.

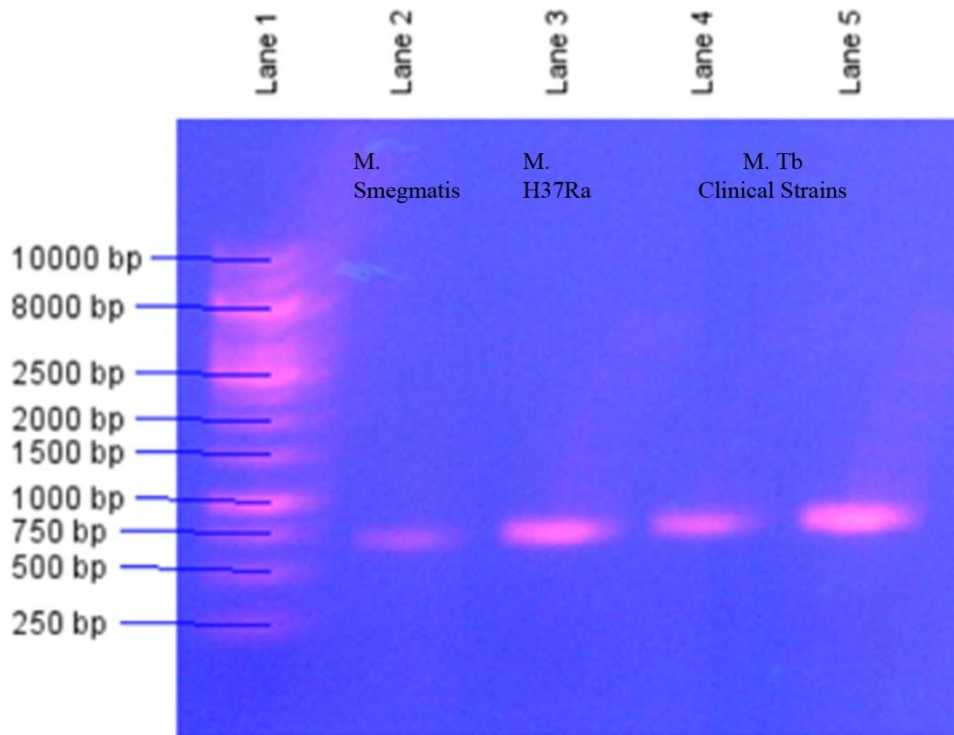


Figure 12. Agarose gel electrophoresis of 16s rDNA amplified from mycobacteria reference and clinical strains

Mycobacteria 16s rDNA PCR amplicons for 2 reference and 2 clinical strains. Amplicons were separated using gel electrophoresis on 0.7% agarose gel, stained with ethidium bromide, and visualized using UV light. PCR resulted in about 700 bp specific amplicons. Figure of 16s rDNA PCR amplicons is a LabImage 1D software processed photo. Lane 1: 10,000 bp DNA ladder. Lane 2: *Mycobacterium smegmatis* 650 bp. Lane 3: *Mycobacterium H37Ra* 700 bp. Lane 4: *Mycobacterium tuberculosis* clinical strain B 750 bp. Lane 5: *Mycobacterium tuberculosis* clinical strain D 790 bp.

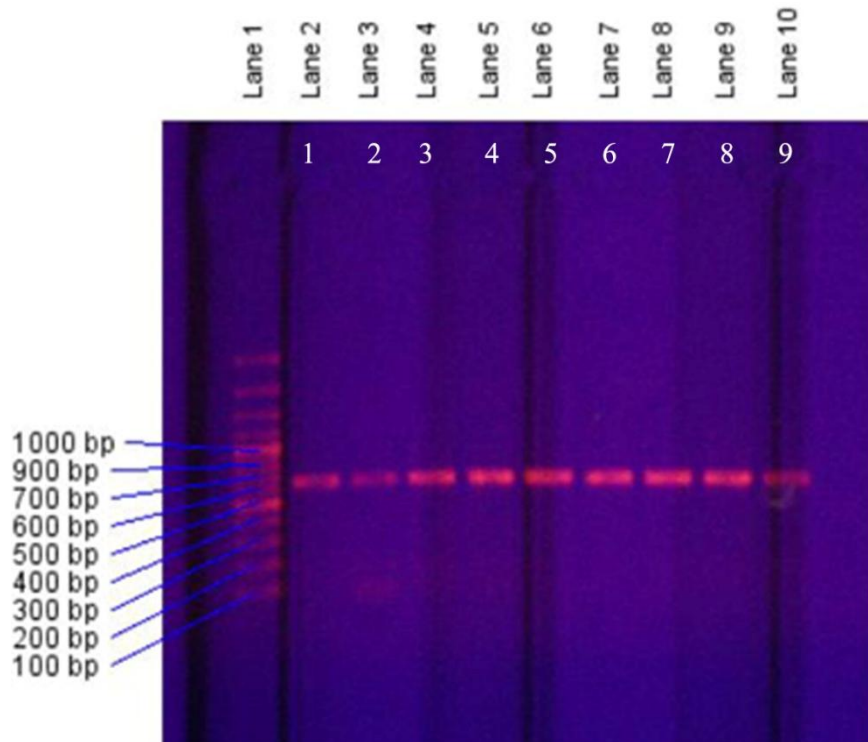


Figure 13. Agarose gel electrophoresis of 16s rDNA amplified from unidentified mycobacterium clinical strains

Mycobacteria 16s rDNA PCR amplicons for 9 unidentified clinical strains. Amplicons were separated using gel electrophoresis on 0.7% agarose gel, stained with ethidium bromide, and visualized using UV light. PCR resulted in about 700 bp specific amplicons. Figure of 16s rDNA PCR amplicon is a LabImage 1D software processed photo. Lane 1: 100 bp DNA ladder. Lane 2: strain 1 (709 bp). Lane 3: strain 2 (727 bp). Lane 4: strain 3 (736 bp). Lane 5: strain 4 (736 bp). Lane 6: strain 5 (727 bp). Lane 7: strain 6 (736 bp). Lane 8: strain 7 (718 bp). Lane 9: strain 8 (736 bp). Lane 10: strain 9 (727 bp).

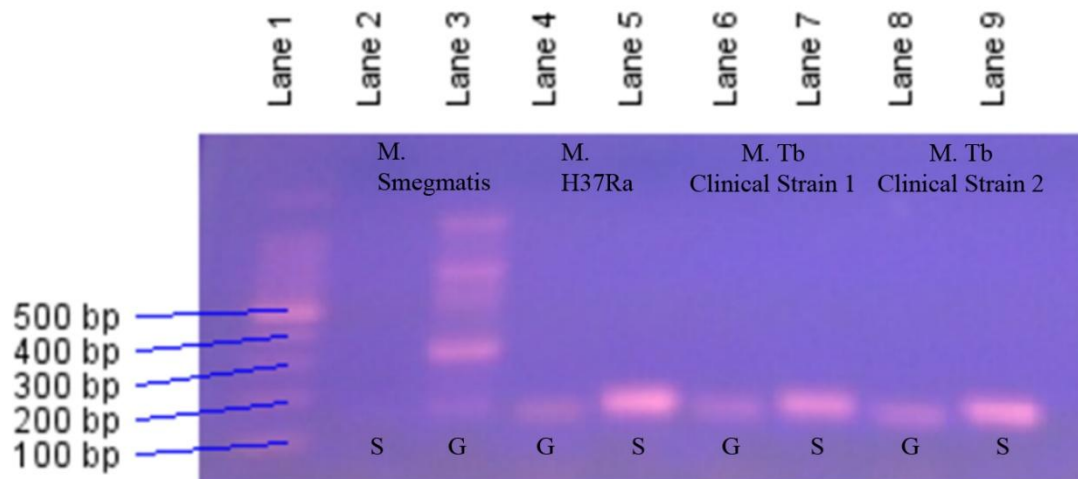


Figure 14. Agarose gel electrophoresis of genus- and species-specific amplicons prepared by semi-nested PCR from mycobacteria reference and clinical strains

Genus and species semi-nested PCR amplicons for 2 reference and 2 clinical mycobacteria strains. Amplicons were separated using gel electrophoresis on 1% agarose gel, stained with ethidium bromide, and visualized using UV light. Semi-nested PCR resulted in genus and species specific regions amplified confirming genus and species oligo-targeters specificity, respectively. Figure of semi-nested PCR is a LabImage 1D software processed photo. Lane 1: 100 bp DNA ladder. Lane 2: *Mycobacterium smegmatis* species (no band). Lane 3: *Mycobacterium smegmatis* genus (173 bp). Lane 4: *Mycobacterium H37Ra* genus (173 bp). Lane 5: *Mycobacterium H37Ra* species (199 bp). Lane 6: *Mycobacterium tuberculosis* clinical strain B genus (186 bp). Lane 7: *Mycobacterium tuberculosis* clinical strain B species (193 bp). Lane 8: *Mycobacterium tuberculosis* clinical strain D genus (167 bp). Lane 9: *Mycobacterium tuberculosis* clinical strain D species (173 bp).

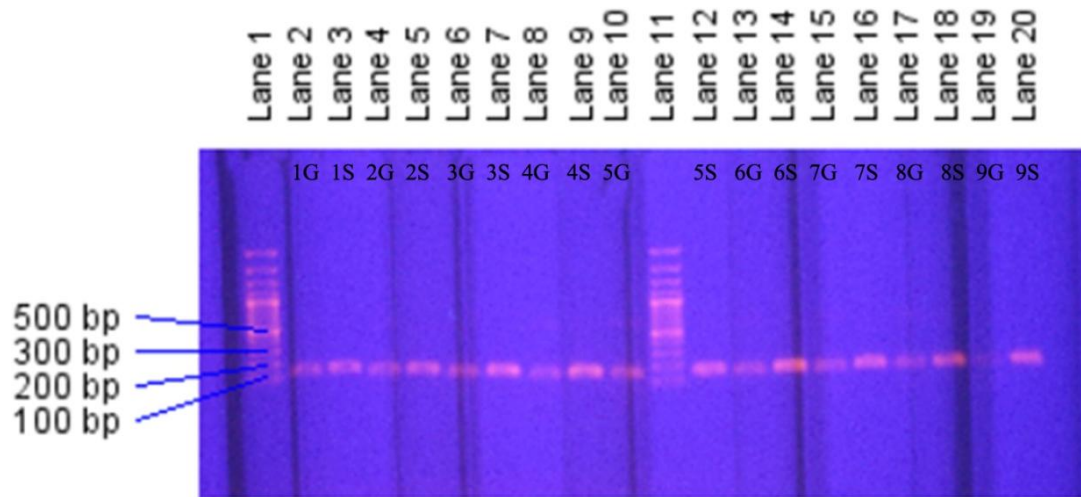


Figure 15. Agarose gel electrophoresis of genus- and species-specific amplicons prepared by semi-nested PCR from unidentified mycobacteria clinical strains

Genus and species semi-nested PCR amplicons for 9 unidentified mycobacteria clinical strains. Amplicons were separated using gel electrophoresis on 1% agarose gel, stained with ethidium bromide, and visualized using UV light. Semi-nested PCR resulted in genus and species specific regions amplified confirming that these 9 mycobacteria strains belong to *M. tuberculosis* complex. Figure of semi-nested PCR is a LabImage 1D software processed photo. Lane 1: 100 bp DNA ladder. Lane 2: strain 1 genus (161 bp). Lane 3: strain 1 species (189 bp). Lane 4: strain 2 genus (168 bp). Lane 5: strain 2 species (178 bp). Lane 6: strain 3 genus (154 bp). Lane 7: strain 3 species (168 bp). Lane 8: strain 4 genus (145 bp). Lane 9: strain 4 species (171 bp). Lane 10: strain 5 genus (160 bp). Lane 11: 100 bp DNA ladder. Lane 12: strain 5 species (186 bp). Lane 13: strain 6 genus (177 bp). Lane 14: strain 6 species (211 bp). Lane 15: strain 7 genus (198 bp). Lane 16: strain 7 species (230 bp). Lane 17: strain 8 genus (225 bp). Lane 18: strain 8 species (249 bp). Lane 19: strain 9 genus (221 bp). Lane 20: strain 9 species (259 bp).

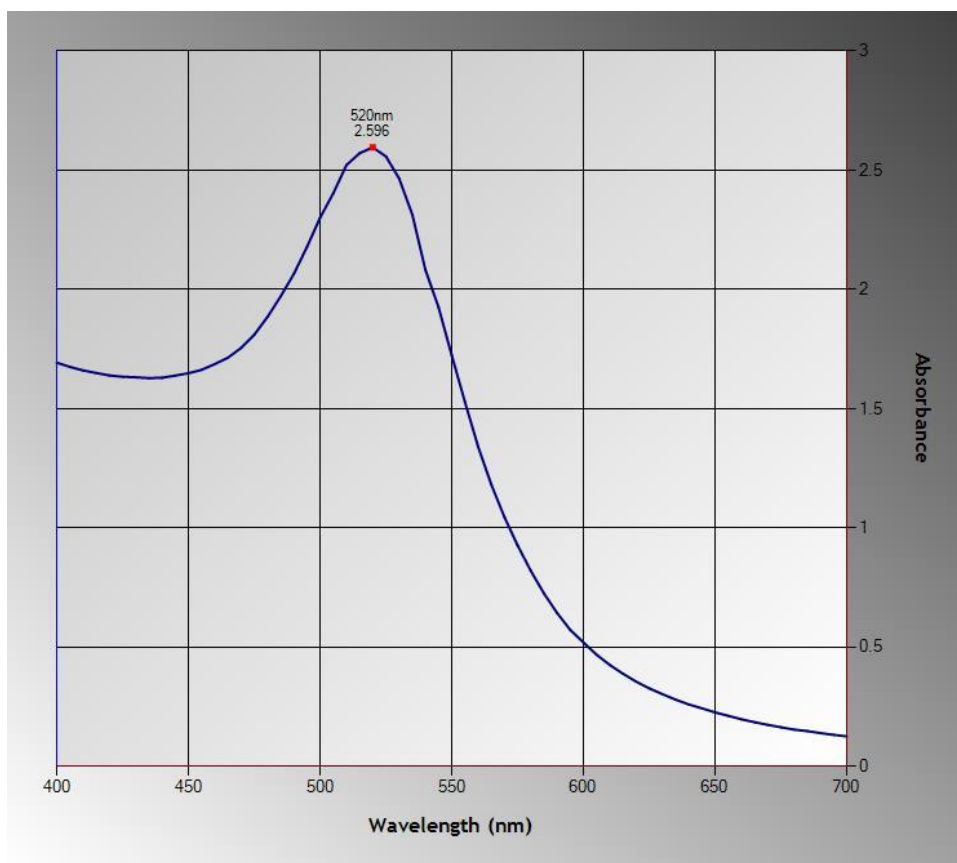


Figure 16. Absorption spectra of synthesized spherical unmodified gold nanoparticles

Spherical gold nanoparticles colloid prepared using citrate reduction method. The method employs the reduction of HAuCl_4 . Synthesized AuNPs have negative surface charges with a diameter of $13 \text{ nm} \pm 2$ and a concentration of 14 nM . Synthesized AuNPs showed a UV-visible absorbance peak at 520 nm .

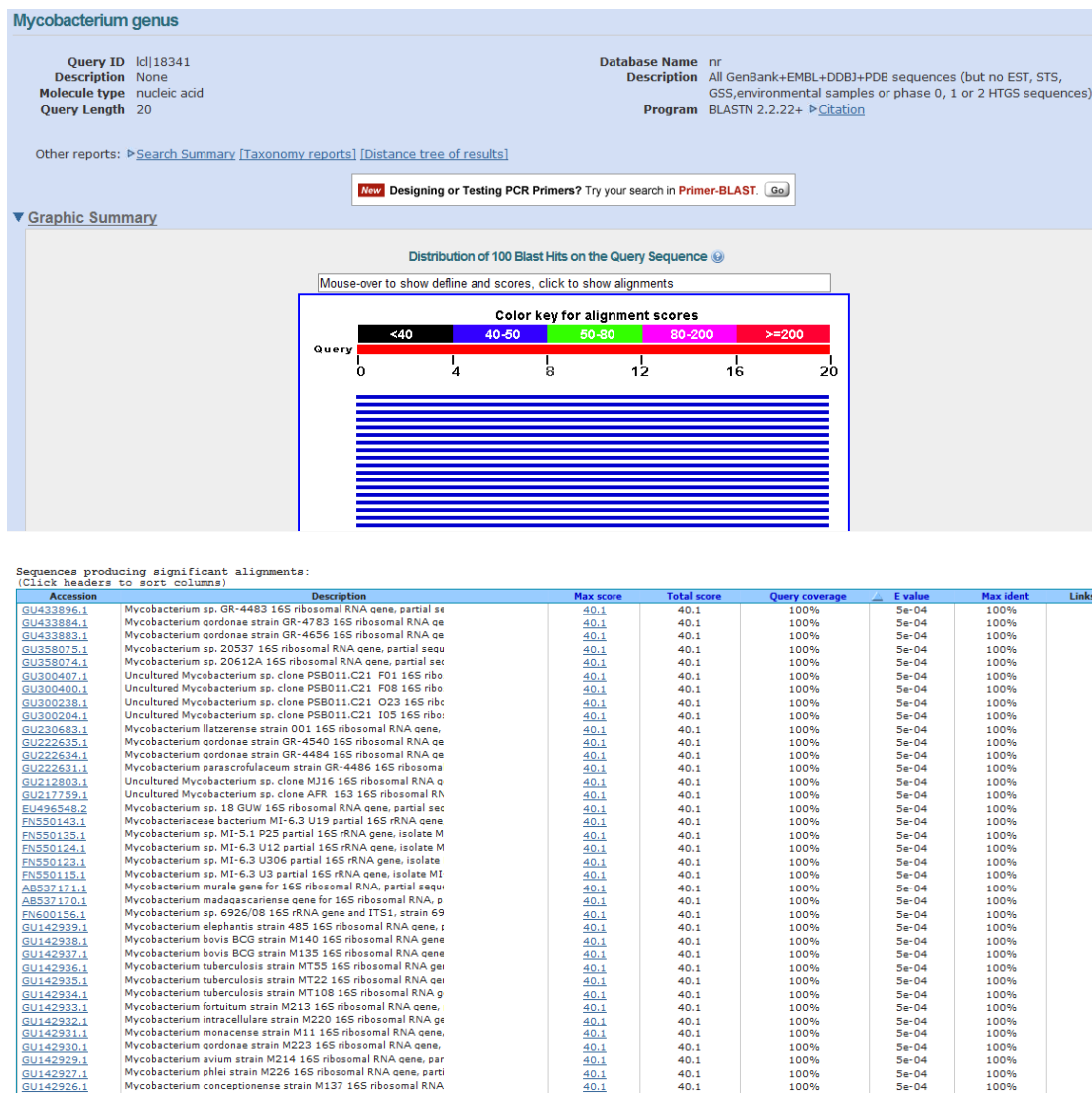
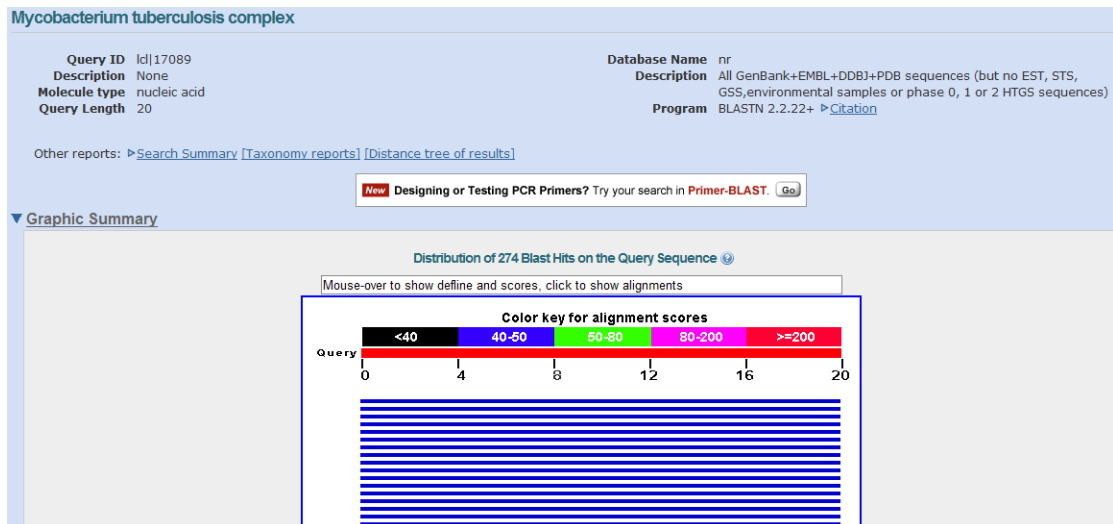


Figure 17. NCBI nucleotide blast results of mycobacterium genus-specific oligo-targeter

Genus oligo-targeter was selected from previous literature based on a conserved 16S rDNA gene segment. The genus mycobacterium oligo-targeter NCBI blastn resulted in (100 blast hits) 100% query coverage for all mycobacteria sequences, confirming selected oligo-targeter specificity to mycobacterium genus.



Sequences producing significant alignments:
 (Click headers to sort columns)

Accession	Description	Max score	Total score	Query coverage	E value	Max ident	Links
GU142938.1	Mycobacterium bovis BCG strain M140 16S ribosomal RNA gene, pa	40.1	40.1	100%	5e-04	100%	
GU142937.1	Mycobacterium bovis BCG strain M135 16S ribosomal RNA gene, pa	40.1	40.1	100%	5e-04	100%	
GU142936.1	Mycobacterium tuberculosis strain MT55 16S ribosomal RNA gene, r	40.1	40.1	100%	5e-04	100%	
GU142935.1	Mycobacterium tuberculosis strain MT22 16S ribosomal RNA gene, r	40.1	40.1	100%	5e-04	100%	
GU142934.1	Mycobacterium tuberculosis strain MT109 16S ribosomal RNA gene, r	40.1	40.1	100%	5e-04	100%	
NR_028879.1	Mycobacterium caprae strain qM-1 16S ribosomal RNA, partial sequ	40.1	40.1	100%	5e-04	100%	
CP001658.1	Mycobacterium tuberculosis KZN 1435, complete genome	40.1	606	100%	5e-04	100%	
AF010918.1	Mycobacterium bovis BCG str. Tokyo 172 DNA, complete genome	40.1	716	100%	5e-04	100%	
FJ468345.1	Mycobacterium tuberculosis strain ATCC 27294 16S ribosomal RNA	40.1	40.1	100%	5e-04	100%	
AB292583.1	Mycobacterium bovis gene for 16S ribosomal RNA, strain: GTC 602	40.1	40.1	100%	5e-04	100%	
CP000717.1	Mycobacterium tuberculosis F11, complete genome	40.1	586	100%	5e-04	100%	
CP000611.1	Mycobacterium tuberculosis H37Ra, complete genome	40.1	604	100%	5e-04	100%	
EF018628.1	Uncultured Mycobacteriaceae bacterium clone Amb_16S_908 16S ri	40.1	40.1	100%	5e-04	100%	
AM408590.1	Mycobacterium bovis BCG Pasteur 1173P2, complete genome	40.1	565	100%	5e-04	100%	
DQ986506.1	Mycobacterium sp. FI-06091 16S ribosomal RNA gene, partial sequ	40.1	40.1	100%	5e-04	100%	
AB268503.1	Mycobacterium shiniukense gene for 16S ribosomal RNA, partial s	40.1	40.1	100%	5e-04	100%	
AM283534.1	Mycobacterium tuberculosis 16S rRNA gene, isolate TB36	40.1	40.1	100%	5e-04	100%	
AM283533.1	Mycobacterium sp. CIPT 19980863 16S rRNA gene, strain 19980863	40.1	40.1	100%	5e-04	100%	
AM283532.1	Mycobacterium sp. CIPT 140070003 16S rRNA gene, strain 199902f	40.1	40.1	100%	5e-04	100%	
AM283531.1	Mycobacterium sp. CIPT 140070002 16S rRNA gene, strain 199917f	40.1	40.1	100%	5e-04	100%	
AM283530.1	Mycobacterium sp. CIPT 140060001 16S rRNA gene, strain 140010f	40.1	40.1	100%	5e-04	100%	
AF627642.2	Mycobacterium sp. CHTN-E 16S ribosomal RNA gene, partial sequer	40.1	40.1	100%	5e-04	100%	
AF000516.2	Mycobacterium tuberculosis CDC1551, complete genome	40.1	647	100%	5e-04	100%	
NR_025249.1	Mycobacterium pinnipedii strain 6482 16S ribosomal RNA, partial se	40.1	40.1	100%	5e-04	100%	
NR_025238.1	Mycobacterium africanum strain ATCC 25420 16S ribosomal RNA, p	40.1	40.1	100%	5e-04	100%	
NR_025234.1	Mycobacterium microti strain ATCC 19422 16S ribosomal RNA, part	40.1	40.1	100%	5e-04	100%	
X58890.1	M.tuberculosis ribosomal RNA operon encoding 16S and 23S ribosor	40.1	40.1	100%	5e-04	100%	
AY673205.1	Mycobacteriaceae bacterium Ellin7039 16S ribosomal RNA gene, pa	40.1	40.1	100%	5e-04	100%	
BX842576.1	Mycobacterium tuberculosis H37Rv complete genome; segment 5/1	40.1	123	100%	5e-04	100%	
BX246338.1	Mycobacterium bovis subsp. bovis AF2122/97 complete genome; se	40.1	125	100%	5e-04	100%	

Figure 18. NCBI nucleotide blast results of *M. tuberculosis* complex-specific oligo-targeter

Species oligo-targeter was selected from previous literature based on a conserved 16S rDNA gene segment. The *Mycobacterium tuberculosis* complex oligo-targeter NCBI blastn resulted in (274 blast hits) 100% query coverage for all *M. tuberculosis* complex members, confirming selected oligo-targeter specificity to *M. tuberculosis* complex.

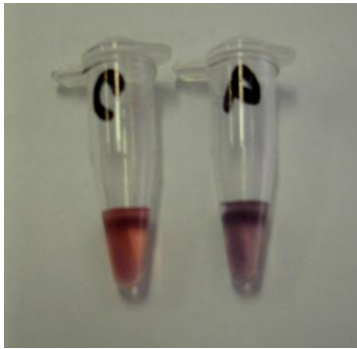


Figure 19. Use of AuNPs for detection of PCR amplicons to differentiate mycobacterium genus from other bacteria

Detection of amplified 16s rDNA PCR amplicons using synthesized AuNPs. Genus and species oligo-targeters used in a concentration ratio of 1:1. PCR amplicons were denatured (95 °C, 30 s) and allowed to anneal (48 °C, 30 s) with genus and species specific oligo-targeters. The hybridization buffer contained NaCl and Tris – HCl. In positive mycobacteria specimen, genus and species oligo-targeters hybridized with their specific regions. AuNPs aggregated change their visual color from red to blue. In negative specimen, genus and species oligo-targeters stabilized AuNPs preventing their aggregation. This first version of the assay differentiated mycobacterium genus from other bacteria. Negative control (left, red) with non specific DNA (*Staph. aureus*). Positive sample (right, blue) with TB DNA.

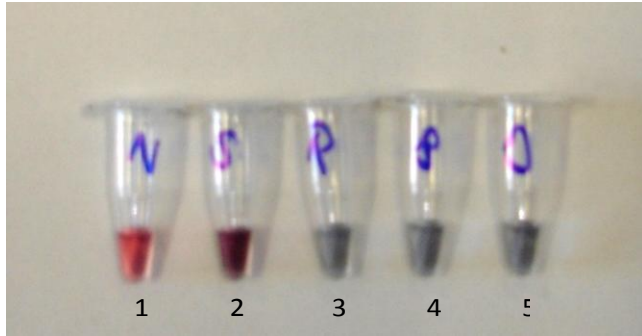


Figure 20. Use of AuNPs for detection of PCR amplicons to differentiate MBTC from mycobacterium genus

Detection of amplified 16s rDNA PCR amplicons using synthesized AuNPs. Genus and species oligo-targeters used in a concentration ratio of 1:2. PCR amplicons were denatured (95 °C, 30 s) and allowed to anneal (48 °C, 30 s) with genus and species specific oligo-targeters. The hybridization buffer contained NaCl and Tris – HCl. In positive mycobacteria specimen, genus and species oligo-targeters hybridized with their specific regions. AuNPs aggregated change their visual color from red to blue. In negative specimen, genus and species oligo-targeters stabilized AuNPs preventing their aggregation. This second version of the assay developed to differentiate *M. tuberculosis* complex from mycobacterium genus. The use of higher concentration of species oligo-targeter prevents hybridization with the target DNA in a *M. smegmatis* specimen. Un-hybridized species oligo-targeter stabilized AuNPs preventing their aggregation. (1) Negative control with non specific DNA. (2) *M. smegmatis* amplified DNA (-ve MTBC). (3) *M. H37Ra* amplified DNA (+ve MBTC). (4) *M. tuberculosis* clinical strain amplified DNA (+ve MBTC). (5) AuNPs *M. tuberculosis* clinical strain amplified DNA (+ve MBTC).

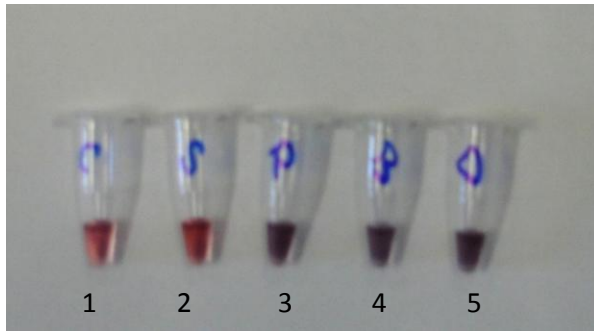


Figure 21. Use of AuNPs for detection of PCR amplicons to differentiate MBTC from mycobacterium genus

Detection of amplified 16s rDNA PCR amplicons using synthesized AuNPs. Genus and species oligo-targeters used in a concentration ratio of 1:3. PCR amplicons were denatured (95 °C, 30 s) and allowed to anneal (48 °C, 30 s) with genus and species specific oligo-targeters. The hybridization buffer contained NaCl and Tris – HCl. In positive mycobacteria specimen, genus and species oligo-targeters hybridized with their specific regions. AuNPs aggregated change their visual color from red to blue. In negative specimen, genus and species oligo-targeters stabilized AuNPs preventing their aggregation. This second version of the assay differentiated *M. tuberculosis* complex from mycobacterium genus, showed positive results for *M. tuberculosis* strains only. The use of higher concentration of species oligo-targeter prevents their hybridization with the target DNA even more in a *M. smegmatis* specimen. Un-hybridized species oligo-targeter stabilized more AuNPs preventing their aggregation. (1) Negative control with non specific DNA. (2) *M. smegmatis* amplified DNA (-ve MTBC). (3) *M. H37Ra* amplified DNA (+ve MBTC). (4) *M. tuberculosis* clinical strain amplified DNA (+ve MBTC). (5) AuNPs *M. tuberculosis* clinical strain amplified DNA (+ve MBTC).

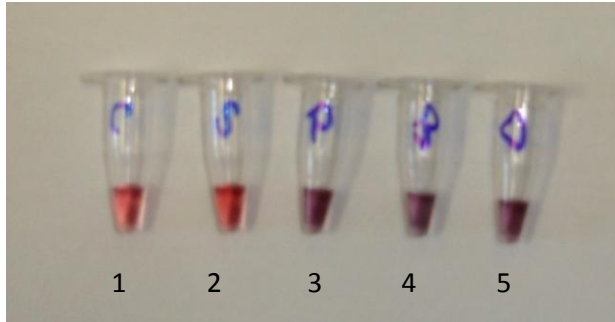


Figure 22. Use of AuNPs for detection of PCR amplicons to differentiate MBTC from mycobacterium genus

Detection of amplified 16s rDNA PCR amplicons using synthesized AuNPs using species oligo-targeter only. PCR amplicons were denatured (95 °C, 30 s) and allowed to anneal (48 °C, 30 s) with species specific oligo-targeter. The hybridization buffer contained NaCl and Tris – HCl. In positive mycobacteria specimen, species oligo-targeter hybridized with its specific region. AuNPs aggregated change their visual color from red to blue. In negative specimen, species oligo-targeter stabilized AuNPs preventing their aggregation. This second version of the assay showed positive results for *M. tuberculosis* strains only, differentiated *M. tuberculosis* complex from mycobacterium genus. The use of only species oligo-targeter prevents hybridization with the target DNA in a *M. smegmatis* specimen. Unhybridized species oligo-targeter stabilized most of AuNPs preventing their aggregation. (1) Negative control with non specific DNA. (2) *M. smegmatis* amplified DNA (-ve MTBC). (3) *M. H37Ra* amplified DNA (+ve MBTC). (4) *M. tuberculosis* clinical strain amplified DNA (+ve MBTC). (5) AuNPs *M. tuberculosis* clinical strain amplified DNA (+ve MBTC).

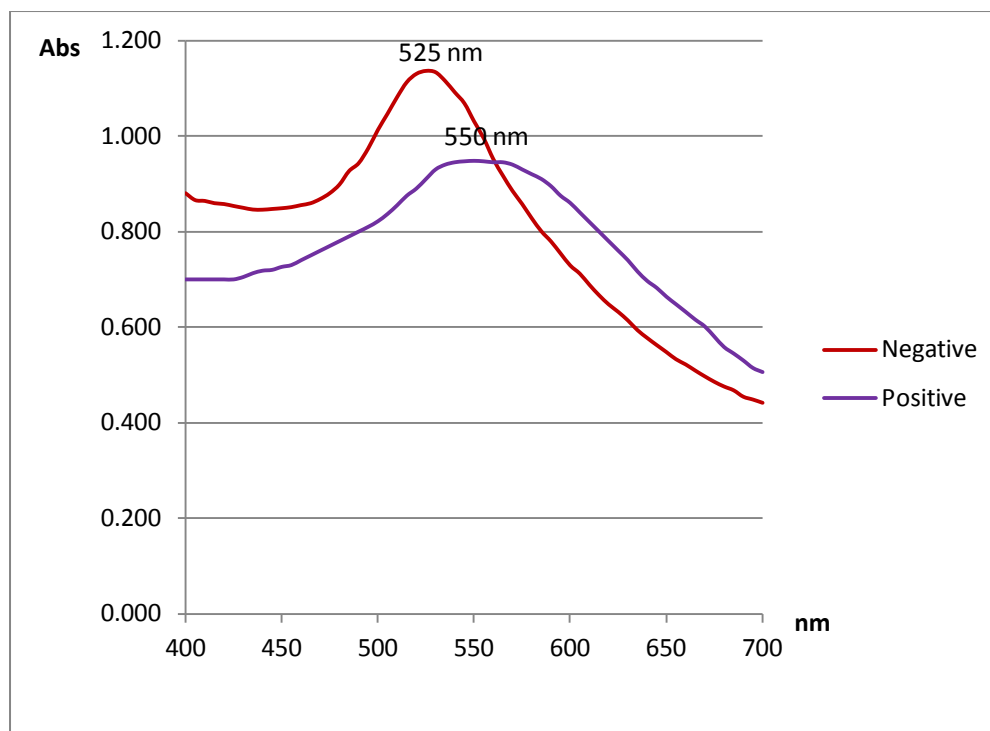


Figure 23. Absorption spectra of AuNPs used for detection of TB 16s rDNA amplicons

The suspected sample denatured and annealed with oligo-targeters in the presence of salt. AuNPs were added for detection. In negative specimen, the target DNA did not hybridize with specific oligo-targeters. Oligo-targeters uncoil sufficiently to get adsorbed on negatively surface charged AuNPs through nitrogenous bases. AuNPs stabilization occurs in the presence of salt, preventing their aggregation and absorbance peak shift. In positive specimens, the target DNA hybridized with specific oligo-targeters. AuNPs aggregated change their visual color from red to blue shifting spectrophotometer absorbance peak. AuNPs absorbance peak shift from 525 nm to 550 nm.

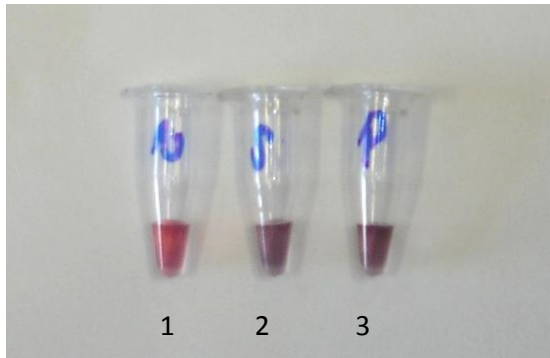


Figure 24. Use of AuNPs for detection of digested genomic DNA to differentiate mycobacterium genus from other bacteria

Genomic DNA was denatured (95 °C, 3 min) and allowed to anneal (48 °C, 1 min) with genus and species specific oligo-targeters. The hybridization buffer contained NaCl and Tris – HCl. In positive mycobacteria specimen, genus and species oligo-targeters hybridized with their specific regions. AuNPs aggregated changing solution color from red to blue. In negative specimen, genus and species oligo-targeters stabilized AuNPs preventing their aggregation. This first version of the assay differentiated mycobacterium genus from other bacteria. (1) Negative control with non specific DNA. (2) *M. smegmatis* digested genomic DNA. (3) *M. H37Ra* digested genomic DNA.

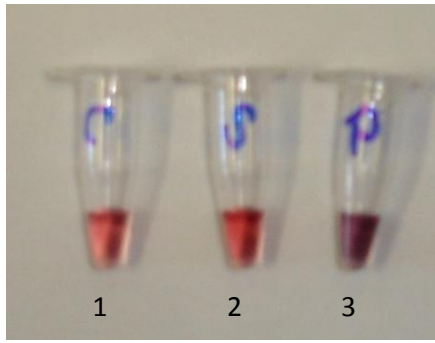


Figure 25. Use of AuNPs for detection of digested genomic DNA to differentiate MTBC from mycobacterium genus

Genomic DNA was denatured (95 °C, 3 min) and allowed to anneal (48 °C, 1 min) with species specific oligo-targeter. The hybridization buffer contained NaCl and Tris – HCl. In positive mycobacteria specimen, species oligo-targeter hybridized with its specific region. AuNPs aggregated change their visual color from red to blue. In negative specimen, species oligo-targeter stabilized AuNPs preventing their aggregation. This second version of the assay showed positive results for *M. tuberculosis* strains only, differentiated *M. tuberculosis* complex from mycobacterium genus. (1) Negative control with non specific DNA. (2) *M. smegmatis* digested genomic DNA. (3) *M. H37Ra* digested genomic DNA.

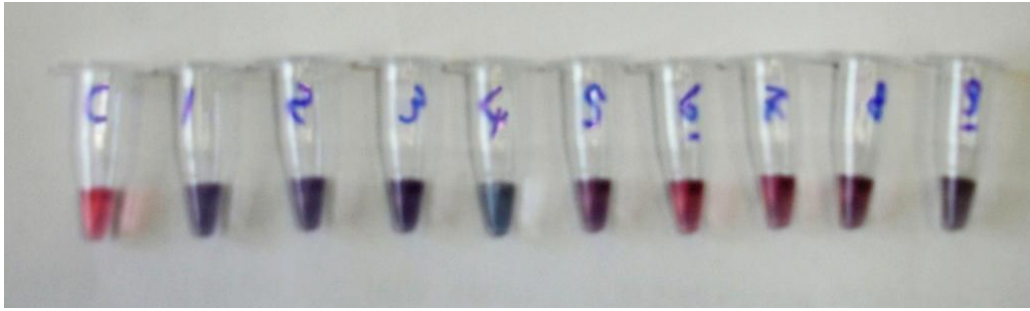


Figure 26. Use of AuNPs for detection of *Bam* HI digested genomic DNA for 9 *M. tuberculosis* clinical specimens

AuNPs detection of *Bam* HI digested genomic DNA using species oligo-targeter only. Genomic DNA was denatured (95 °C, 3 min) and allowed to anneal (48 °C, 1 min) with species specific oligo-targeter. This second version of the assay showed positive results for *M. tuberculosis* strains. Negative control (far left tube, red). Tubes (1 to 9): *M. tuberculosis* digested genomic DNA with different DNA concentrations.



Figure 27. Confirmation of AuNPs detection of *Bam* HI digested genomic DNA for 14 *M. tuberculosis* clinical specimens

AuNPs detection of *Bam* HI digested genomic DNA was done using species specific oligo-targeter only. Genomic DNA was denatured (95 °C, 3 min) and allowed to anneal (48 °C, 1 min) with species specific oligo-targeter. This second version of the assay confirmed the nano-gold assay sensitivity. Negative control (upper row, far left tube) with *Mycobacterium smegmatis* digested genomic DNA. Tubes 11 to 24: *M. tuberculosis* digested genomic DNA with a standardized DNA concentration (~ 80 ng).

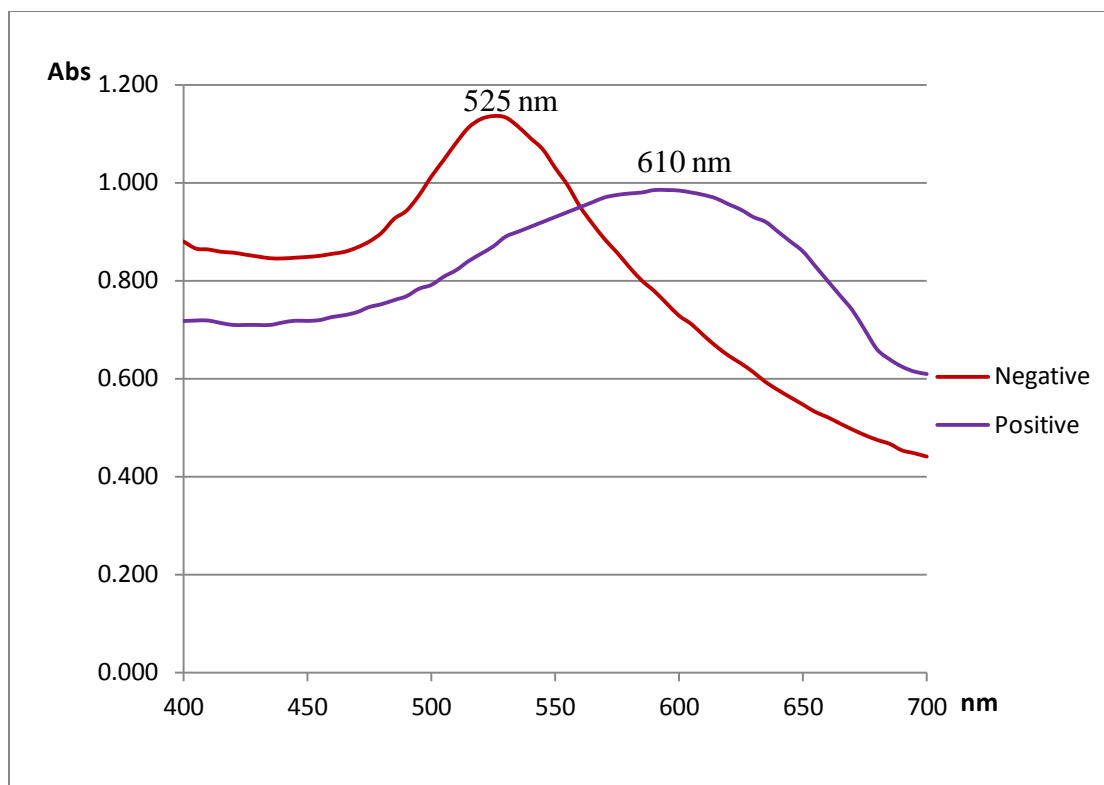


Figure 28. Absorption spectra of AuNPs in samples containing mycobacteria digested genomic DNA

The suspected sample denatured and annealed with oligo-targeters in the presence of salt. AuNPs were added for detection. In negative specimen, the target DNA did not hybridize with specific oligo-targeters. Oligo-targeters uncoil sufficiently to get adsorbed on negatively surface charged AuNPs through nitrogenous bases. AuNPs stabilization occurs in the presence of salt, preventing their aggregation and absorbance peak shift. In positive specimens, the target DNA hybridized with specific oligo-targeters. AuNPs aggregated change their visual color from red to blue shifting spectrophotometer absorbance peak. AuNPs absorbance peak shifted from 525 nm to 610 nm.



Figure 29. Nano-gold assay detection limit for *Mycobacterium H37Ra* PCR amplicons

Mycobacterium H37Ra amplicons were serially diluted and tested by the TB nanogold assay. The ability of the oligo-targeter to find the target decreased by increasing dilution. AuNPs induced complete aggregation in the first 3 reactions (R1-R3), partial aggregation in R4 and R5 reactions, and no aggregation in the last reaction (R6). R1-R6: *Mycobacterium H37Ra* samples contain amplified DNA with different DNA quantities: (R1) 14 ng, (R2) 7 ng, (R3) 3.5 ng, (R4) 1.75 ng, (R5) 0.857 ng, and (R6) 0.4 ng.

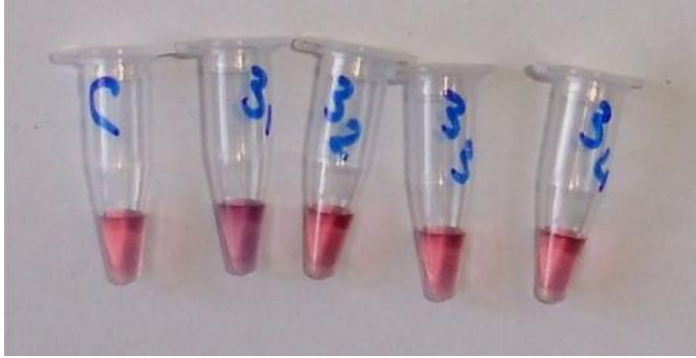


Figure 30. Nano-gold assay detection limit for mycobacterium digested genomic DNA from clinical strains

Digested genomic DNA detection limit for *Mycobacterium tuberculosis* clinical specimen. Mycobacterium genomic DNA was serially diluted and allowed for detection. The first reaction was positive while the rest of dilutions gave negative aggregation. (C) Negative control. (3) *Mycobacterium tuberculosis* clinical strain number 3 with different DNA quantities: (3₁) 40 ng, (3₂) 30 ng, (3₃) 20 ng, (3₄) 10 ng.

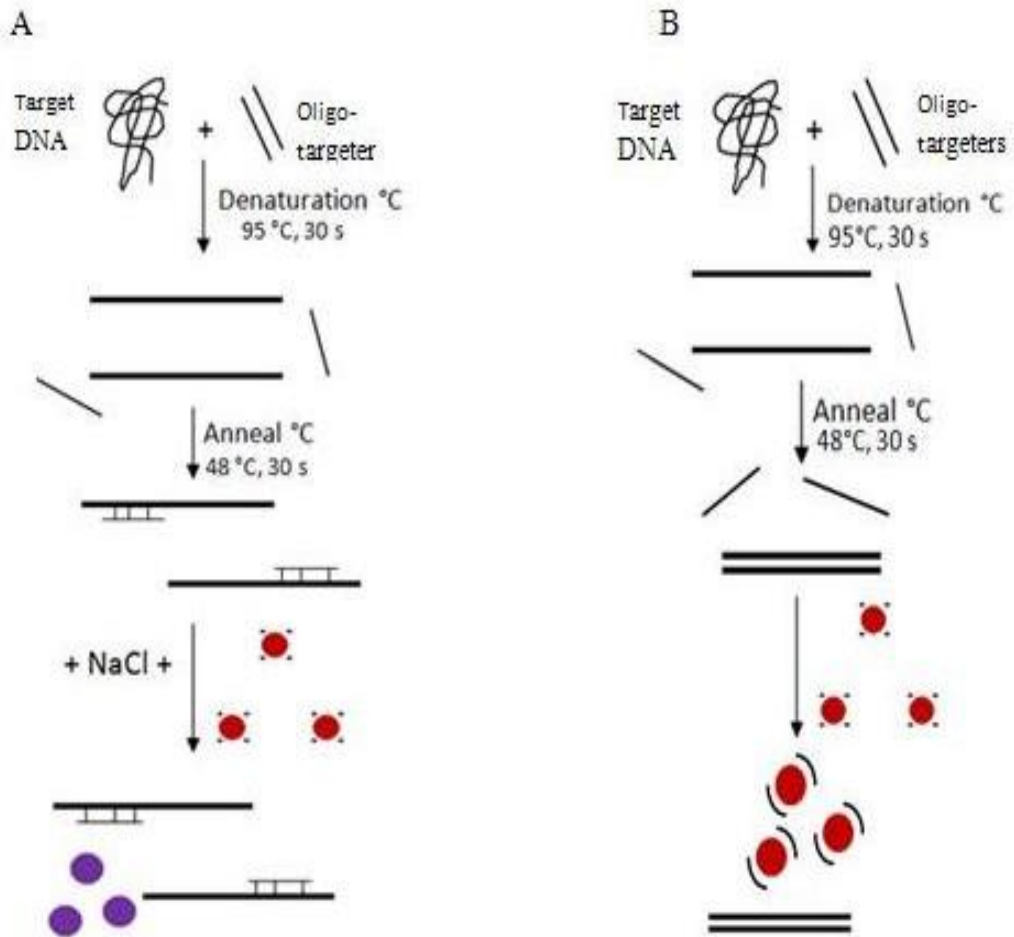


Figure 31. Detection principle of unmodified gold nanoparticles

In unmodified AuNPs detection, DNA is denatured and annealed to specific oligo-targeters. The hybridization buffer mostly includes salts. Then AuNPs are added to the reaction mixture. (A) In the presence of positive target, oligo-targeters hybridize and become unavailable to protect and stabilize AuNPs. Presence of salt causes AuNPs to aggregate and the solution changes from red to blue. (B) In the presence of no or non-specific target, oligo-targeters uncoil and get adsorbed via their nitrogenous base side to the negatively charged AuNP surface. AuNPs become stabilized and do not aggregate; solution color remains red.

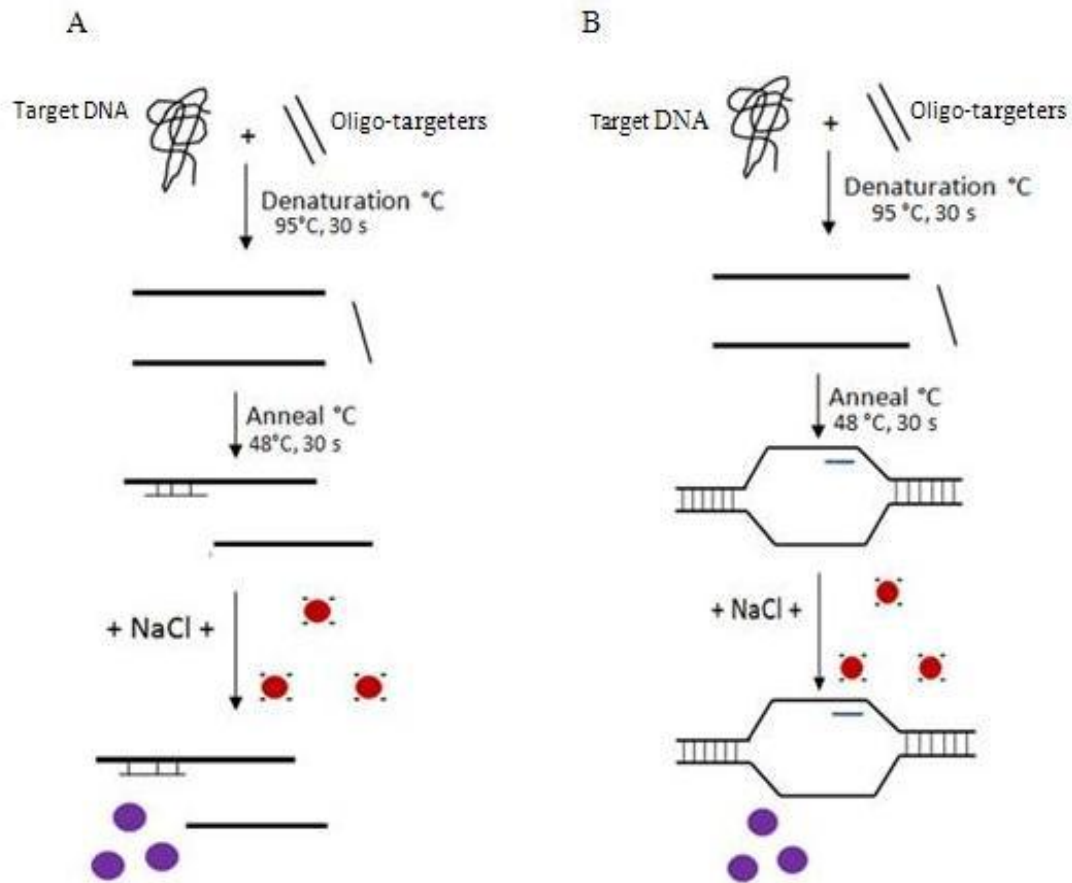


Figure 32. Possible hypothetical explanations for the use of a single, rather than two, oligo-targeter in the TB nano-gold assay

Gold nanoparticles detection principle contradicts with using single oligo-targeter. (A) The first possible explanation is that long (target) ssDNA do not stabilize AuNPs. AuNPs induced aggregation changing their visual color from red to blue. (B) The second probable explanation is that DNA target may denatures and/or anneals in a replication bubble manner. Thus, the presence of one/two oligo-targeter/s to anneal with the target in a replication fork would not stabilize AuNPs allowing for their salt-induced aggregation.

CHAPTER 9: References

1. WHO: **Global tuberculosis control 2011**. 2011. [website was last accessed on Jan 15, 2012].
2. WHO: **Egypt tuberculosis profile**. 2011. [website was last accessed on Jan 15, 2012].
3. Gordon SV, Bottai D, Simeone R, Stinear TP, Brosch R: **Pathogenicity in the tubercle bacillus: molecular and evolutionary determinants**. *Bioessays* 2009, **31**:378-388.
4. Al-Zamel FA: **Detection and diagnosis of Mycobacterium tuberculosis**. *Expert Rev Anti Infect Ther* 2009, **7**:1099-1108.
5. Parkash O, Singh BP, Pai M: **Regions of Differences Encoded Antigens as Targets for Immunodiagnosis of Tuberculosis in Humans**. *Scandinavian Journal of Immunology* 2009, **70**:345-357.
6. Abdallah AM, van Pittius NCG, Champion PAD, Cox J, Luirink J, Vandenbroucke-Grauls CMJE, Appelmelk BJ, Bitter W: **Type VII secretion "mycobacteria show the way"**. In *Nature Reviews Microbiology*, vol. 5. pp. 883-891: Nature Publishing Group; 2007:883-891.
7. Pym AS, Brodin P, Brosch R, Huerre M, Cole ST: **Loss of RD1 contributed to the attenuation of the live tuberculosis vaccines Mycobacterium bovis BCG and Mycobacterium microti**. *Mol Microbiol* 2002, **46**:709-717.
8. WHO: **Tuberculosis**. vol. Fact sheet N 104: Media centre; 2010.
9. AHN, #160, H. C, CHOI, Jin-Woo, BEAUCAGE, Gregory, NEVIN, H. J, LEE, et al: **Disposable Smart lab on a chip for point-of-care clinical diagnostics**. New York, NY, ETATS-UNIS: Institute of Electrical and Electronics Engineers; 2004.
10. TB S: **Advocacy, Communication and Social Mobilization**. WHO; 2012.
11. WHO T: **Diagnostics for tuberculosis Global demand and market potential**. 2006.
12. WHO STP: **New laboratory diagnostic tools for tuberculosis control**. 2008.
13. Glaziou P, Floyd K, Raviglione M: **Global burden and epidemiology of tuberculosis**. *Clin Chest Med* 2009, **30**:621-636, vii.
14. Tiwari RP, Hattikudur NS, Bharmal RN, Kartikeyan S, Deshmukh NM, Bisen PS: **Modern approaches to a rapid diagnosis of tuberculosis: promises and challenges ahead**. *Tuberculosis (Edinb)* 2007, **87**:193-201.
15. Venkataraman P, Herbert D, Paramasivan CN: **Evaluation of the BACTEC radiometric method in the early diagnosis of tuberculosis**. *Indian J Med Res* 1998, **108**:120-127.
16. Ahmad S, Mokaddas E: **Recent advances in the diagnosis and treatment of multidrug-resistant tuberculosis**. *Respir Med* 2009, **103**:1777-1790.
17. Neonakis IK, Gitti Z, Krambovitis E, Spandidos DA: **Molecular diagnostic tools in mycobacteriology**. *J Microbiol Methods* 2008, **75**:1-11.
18. Bergmann JS, Woods GL: **Clinical evaluation of the Roche AMPLICOR PCR Mycobacterium tuberculosis test for detection of M. tuberculosis in respiratory specimens**. *J Clin Microbiol* 1996, **34**:1083-1085.
19. Palomino JC: **Molecular detection, identification and drug resistance detection in Mycobacterium tuberculosis**. *FEMS Immunol Med Microbiol* 2009, **56**:103-111.
20. Liu W-T: **Nanoparticles and their biological and environmental applications**. *Journal of Bioscience and Bioengineering* 2006, **102**:1-7.
21. Sanvicens N, Marco MP: **Multifunctional nanoparticles - properties and prospects for their use in human medicine**. *Trends in Biotechnology* 2008, **26**:425-433.
22. de Dios AS, Díaz-García ME: **Multifunctional nanoparticles: Analytical prospects**. *Analytica Chimica Acta* 2010, **666**:1-22.
23. Azzazy HME, Mansour MMH: **In vitro diagnostic prospects of nanoparticles**. *Clinica Chimica Acta* 2009, **403**:1-8.
24. Azzazy HM, Mansour MM, Kazmierczak SC: **Nanodiagnosics: a new frontier for clinical laboratory medicine**. *Clin Chem* 2006, **52**:1238-1246.

25. Jain KK: **Nanotechnology in clinical laboratory diagnostics.** *Clin Chim Acta* 2005, **358**:37-54.
26. Russ Algar W, Massey M, Krull UJ: **The application of quantum dots, gold nanoparticles and molecular switches to optical nucleic-acid diagnostics.** *TrAC Trends in Analytical Chemistry* 2009, **28**:292-306.
27. Huang X, El-Sayed MA: **Gold nanoparticles: Optical properties and implementations in cancer diagnosis and photothermal therapy.** *Journal of Advanced Research* 2010, **1**:13-28.
28. Radwan SH, Azzazy HM: **Gold nanoparticles for molecular diagnostics.** *Expert Rev Mol Diagn* 2009, **9**:511-524.
29. Jain PK, El-Sayed IH, El-Sayed MA: **Au nanoparticles target cancer.** *Nano Today* 2007, **2**:18-29.
30. Baptista P, Pereira E, Eaton P, Doria G, Miranda A, Gomes I, Quaresma P, Franco R: **Gold nanoparticles for the development of clinical diagnosis methods.** *Anal Bioanal Chem* 2008, **391**:943-950.
31. Huang X, Jain PK, El-Sayed IH, El-Sayed MA: **Gold nanoparticles: interesting optical properties and recent applications in cancer diagnostics and therapy.** *Nanomedicine* 2007, **2**:681-693.
32. Jain PK, Lee KS, El-Sayed IH, El-Sayed MA: **Calculated absorption and scattering properties of gold nanoparticles of different size, shape, and composition: applications in biological imaging and biomedicine.** *J Phys Chem B* 2006, **110**:7238-7248.
33. *Tuberculosis 2007 from basic science to patient care.* First edn; 2007.
34. Soini H, Musser JM: **Molecular diagnosis of mycobacteria.** *Clin Chem* 2001, **47**:809-814.
35. Saiman L: **The mycobacteriology of non-tuberculous mycobacteria.** *Paediatric Respiratory Reviews* 2004, **5**:S221-S223.
36. McGrath EE, Anderson PB: **The therapeutic approach to non-tuberculous mycobacterial infection of the lung.** *Pulmonary Pharmacology & Therapeutics* 2010, **In Press, Uncorrected Proof.**
37. Piersimoni C, Scarparo C: **Pulmonary infections associated with non-tuberculous mycobacteria in immunocompetent patients.** *The Lancet Infectious Diseases* 2008, **8**:323-334.
38. Shin JH, Lee EJ, Lee HR, Ryu SM, Kim HR, Chang CL, Kim YJ, Lee JN: **Prevalence of non-tuberculous mycobacteria in a hospital environment.** *Journal of Hospital Infection* 2007, **65**:143-148.
39. Hussein Z, Landt O, Wirths B, Wellinghausen N: **Detection of non-tuberculous mycobacteria in hospital water by culture and molecular methods.** *International Journal of Medical Microbiology* 2009, **299**:281-290.
40. Thomson RM: **Changing epidemiology of pulmonary nontuberculous mycobacteria infections.** *Emerg Infect Dis*, **16**:1576-1583.
41. Winthrop KL, Varley CD, Ory J, Cassidy PM, Hedberg K: **Pulmonary disease associated with nontuberculous mycobacteria, Oregon, USA.** *Emerg Infect Dis*, **17**:1760-1761.
42. Niemann S, Richter E, Rusch-Gerdes S: **Differentiation among Members of the Mycobacterium tuberculosis Complex by Molecular and Biochemical Features: Evidence for Two Pyrazinamide-Susceptible Subtypes of M. bovis.** *J Clin Microbiol* 2000, **38**:152-157.
43. Xavier Emmanuel F, Seagar AL, Doig C, Rayner A, Claxton P, Laurenson I: **Human and animal infections with Mycobacterium microti, Scotland.** *Emerg Infect Dis* 2007, **13**:1924-1927.

44. Rodr, guez E, nchez LP, rez S, Herrera L, Jim, nez MS, Samper S, Iglesias MJ: **Human tuberculosis due to Mycobacterium bovis and M. caprae in Spain, 2004-2007.** *The International Journal of Tuberculosis and Lung Disease* 2009, **13**:1536-1541.
45. Meyer CG, Scarisbrick G, Niemann S, Browne ENL, Chinbuah MA, Gyapong J, Osei I, Owusu-Dabo E, Kubica T, Rüsç-Gerdes S, et al: **Pulmonary tuberculosis: Virulence of Mycobacterium africanum and relevance in HIV co-infection.** *Tuberculosis* 2008, **88**:482-489.
46. Wells AQ: **The murine type of tubercle bacillus (the vole acid-fast bacillus).** *Sir William Dunn School of Pathology, University of Oxford, Oxford, United Kingdom* 1946.
47. Frank W, Reisinger EC, Brandt-Hamerla W, Schwede I, Handrick W: **Mycobacterium microti--pulmonary tuberculosis in an immunocompetent patient.** *Wien Klin Wochenschr* 2009, **121**:282-286.
48. Smith NH, Crawshaw T, Parry J, Birtles RJ: **Mycobacterium microti: More Diverse than Previously Thought.** *J Clin Microbiol* 2009, **47**:2551-2559.
49. Prodinger WM, Brandstatter A, Naumann L, Pacciarini M, Kubica T, Boschirolì ML, Aranaz A, Nagy G, Cvetnic Z, Ocepek M, et al: **Characterization of Mycobacterium caprae Isolates from Europe by Mycobacterial Interspersed Repetitive Unit Genotyping.** *J Clin Microbiol* 2005, **43**:4984-4992.
50. Bezos J, de Juan L, Romero B, Álvarez J, Mazzucchelli F, Mateos A, Domínguez L, Aranaz A: **Experimental infection with Mycobacterium caprae in goats and evaluation of immunological status in tuberculosis and paratuberculosis co-infected animals.** *Veterinary Immunology and Immunopathology* 2010, **133**:269-275.
51. Goh KS, Legrand E, Sola C, Rastogi N: **Rapid differentiation of "Mycobacterium canettii" from other Mycobacterium tuberculosis complex organisms by PCR-restriction analysis of the hsp65 gene.** *J Clin Microbiol* 2001, **39**:3705-3708.
52. Bigi F, Garcia-Pelayo MC, Nuñez-García J, Peralta A, Caimi KC, Golby P, Hinds J, Cataldi A, Gordon SV, Romano MI: **Identification of genetic markers for Mycobacterium pinnipedii through genome analysis.** *FEMS Microbiology Letters* 2005, **248**:147-152.
53. Kiers A, Klarenbeek A, Mendelst B, Van Soolingen D, Koeter G: **Transmission of Mycobacterium pinnipedii to humans in a zoo with marine mammals.** *Int J Tuberc Lung Dis* 2008, **12**:1469-1473.
54. Vankayalapati R, Barnes PF: **Innate and adaptive immune responses to human Mycobacterium tuberculosis infection.** *Tuberculosis* 2009, **89**:S77-S80.
55. Hernandez-Pando R, Orozco H, Aguilar D: **Factors that deregulate the protective immune response in tuberculosis.** *Archivum Immunologiae et Therapiae Experimentalis* 2009, **57**:355-367.
56. Apt A, Kondratieva T: **Tuberculosis: Pathogenesis, immune response, and host genetics.** *Molecular Biology* 2008, **42**:784-793.
57. Fallahi-Sichani M, Schaller MA, Kirschner DE, Kunkel SL, Linderman JJ: **Identification of Key Processes that Control Tumor Necrosis Factor Availability in a Tuberculosis Granuloma.** *PLoS Comput Biol* 2010, **6**:e1000778.
58. Scherr N, Jayachandran R, Mueller P, Pieters J: **Interference of Mycobacterium tuberculosis with macrophage responses.** *Indian J Exp Biol* 2009, **47**:401-406.
59. Saunders BM, Britton WJ: **Life and death in the granuloma: immunopathology of tuberculosis.** *Immunol Cell Biol* 2007, **85**:103-111.
60. Kaufmann SHE: **HOW CAN IMMUNOLOGY CONTRIBUTE TO THE CONTROL OF TUBERCULOSIS?** In *Nature Reviews Immunology*, vol. 1. pp. 20: Nature Publishing Group; 2001:20.

61. Bezuidenhout J, Roberts T, Muller L, van Helden P, Walzl G: **Pleural Tuberculosis in Patients with Early HIV Infection Is Associated with Increased TNF-Alpha Expression and Necrosis in Granulomas.** *PLoS One* 2009, **4**:e4228.
62. Grange JM: **Virulence of *Mycobacterium tuberculosis*.** *FEMS Microbiology Letters* 1985, **32**:55-60.
63. Smith I: ***Mycobacterium tuberculosis* pathogenesis and molecular determinants of virulence.** *Clin Microbiol Rev* 2003, **16**:463-496.
64. Tortoli E, Mandler F, Tronci M, Penati V, Sbaraglia G, Costa D, Montini G, Predominato M, Riva R, Tosi CP, et al: **Multicenter evaluation of mycobacteria growth indicator tube (MGIT) compared with the BACTEC radiometric method, BBL biphasic growth medium and Lowenstein-Jensen medium.** *Clin Microbiol Infect* 1997, **3**:468-473.
65. Isenberg HD, D'Amato RF, Heifets L, Murray PR, Scardamaglia M, Jacobs MC, Alperstein P, Niles A: **Collaborative feasibility study of a biphasic system (Roche Septi-Chek AFB) for rapid detection and isolation of mycobacteria.** *J Clin Microbiol* 1991, **29**:1719-1722.
66. Du R, Chen B, Guo L, Li Y, Xie J, Wang G, Zhou H: **[Identification of *Mycobacterium* species using reversed-phase high performance liquid chromatographic analysis of mycolic acid].** *Se Pu* 2008, **26**:534-539.
67. Kalantri S, Pai M, Pascopella L, Riley L, Reingold A: **Bacteriophage- based tests for the detection of *Mycobacterium tuberculosis* in clinical specimens: a systematic review and meta- analysis.** *BMC Infect Dis* 2005, **5**:59.
68. Gali N, Dominguez J, Blanco S, Prat C, Quesada MD, Matas L, Ausina V: **Utility of an in-house mycobacteriophage-based assay for rapid detection of rifampin resistance in *Mycobacterium tuberculosis* clinical isolates.** *J Clin Microbiol* 2003, **41**:2647-2649.
69. Singh S, Saluja TP, Kaur M, Khilnani GC: **Comparative evaluation of FASTPlaque assay with PCR and other conventional in vitro diagnostic methods for the early detection of pulmonary tuberculosis.** *J Clin Lab Anal* 2008, **22**:367-374.
70. LALVANI A, PATHAN AA, McSHANE H, WILKINSON RJ, LATIF M, CONLON CP, PASVOL G, HILL AV: **Rapid Detection of *Mycobacterium tuberculosis* Infection by Enumeration of Antigen-specific T Cells.** *American Journal of Respiratory and Critical Care Medicine* 2001, **163**:824-828.
71. Flaws LBML: *Molecular diagnostics: fundamentals, methods, and clinical applications.* 2007.
72. Tortoli E, Tronci M, Tosi CP, Galli C, Lavinia F, Natili S, Goglio A: **Multicenter evaluation of two commercial amplification kits (Amplicor, Roche and LCx, Abbott) for direct detection of *Mycobacterium tuberculosis* in pulmonary and extrapulmonary specimens.** *Diagn Microbiol Infect Dis* 1999, **33**:173-179.
73. Piersimoni C, Callegaro A, Scarparo C, Penati V, Nista D, Bornigia S, Lacchini C, Scagnelli M, Santini G, De Sio G: **Comparative evaluation of the new gen-probe *Mycobacterium tuberculosis* amplified direct test and the semiautomated abbott LCx *Mycobacterium tuberculosis* assay for direct detection of *Mycobacterium tuberculosis* complex in respiratory and extrapulmonary specimens.** *J Clin Microbiol* 1998, **36**:3601-3604.
74. Fadda G, Ardito F, Sanguinetti M, Posteraro B, Ortona L, Chezzi C, Polonelli L, Dettori G, Conti S, Fanti F, Galli C: **Evaluation of the Abbott LCx *Mycobacterium tuberculosis* assay in comparison with culture methods in selected Italian patients.** *New Microbiol* 1998, **21**:97-103.
75. Kim H, Kim SH, Shim TS, Kim MN, Bai GH, Park YG, Lee SH, Cha CY, Kook YH, Kim BJ: **PCR restriction fragment length polymorphism analysis (PRA)-algorithm targeting**

- 644 bp Heat Shock Protein 65 (hsp65) gene for differentiation of Mycobacterium spp.** *J Microbiol Methods* 2005, **62**:199-209.
76. Mun HS, Kim HJ, Oh EJ, Kim H, Park YG, Bai GH, Do J, Cha CY, Kook YH, Kim BJ: **Direct application of A_{va}II PCR restriction fragment length polymorphism analysis (A_{va}II PRA) targeting 644 bp heat shock protein 65 (hsp65) gene to sputum samples.** *Microbiol Immunol* 2007, **51**:105-110.
 77. Kim BJ, Lee KH, Park BN, Kim SJ, Park EM, Park YG, Bai GH, Kook YH: **Detection of rifampin-resistant Mycobacterium tuberculosis in sputa by nested PCR-linked single-strand conformation polymorphism and DNA sequencing.** *J Clin Microbiol* 2001, **39**:2610-2617.
 78. Kim SY, Park YJ, Song E, Jang H, Kim C, Yoo J, Kang SJ: **Evaluation of the CombiChip Mycobacteria Drug-Resistance detection DNA chip for identifying mutations associated with resistance to isoniazid and rifampin in Mycobacterium tuberculosis.** *Diagn Microbiol Infect Dis* 2006, **54**:203-210.
 79. Hall L, Doerr KA, Wohlfiel SL, Roberts GD: **Evaluation of the MicroSeq system for identification of mycobacteria by 16S ribosomal DNA sequencing and its integration into a routine clinical mycobacteriology laboratory.** *J Clin Microbiol* 2003, **41**:1447-1453.
 80. Aryan E, Makvandi M, Farajzadeh A, Huygen K, Bifani P, Mousavi S-L, Fateh A, Jelodar A, Gouya M-M, Romano M: **A novel and more sensitive loop-mediated isothermal amplification assay targeting IS6110 for detection of Mycobacterium tuberculosis complex.** *Microbiological Research* 2009, **In Press, Corrected Proof**.
 81. Jing G, Polaczyk A, Oerther DB, Papautsky I: **Development of a microfluidic biosensor for detection of environmental mycobacteria.** *Sensors and Actuators B: Chemical* 2007, **123**:614-621.
 82. Ren J, He F, Yi S, Cui X: **A new MSPQC for rapid growth and detection of Mycobacterium tuberculosis.** *Biosensors and Bioelectronics* 2008, **24**:403-409.
 83. Chang HJ, Huang MY, Yeh CS, Chen CC, Yang MJ, Sun CS, Lee CK, Lin SR: **Rapid diagnosis of tuberculosis directly from clinical specimens by gene chip.** *Clin Microbiol Infect* 2009.
 84. Baptista PV, Koziol-Montewka M, Paluch-Oles J, Doria G, Franco R: **Gold-nanoparticle-probe-based assay for rapid and direct detection of Mycobacterium tuberculosis DNA in clinical samples.** *Clin Chem* 2006, **52**:1433-1434.
 85. Soo PC, Horng YT, Chang KC, Wang JY, Hsueh PR, Chuang CY, Lu CC, Lai HC: **A simple gold nanoparticle probes assay for identification of Mycobacterium tuberculosis and Mycobacterium tuberculosis complex from clinical specimens.** *Mol Cell Probes* 2009, **23**:240-246.
 86. Liandris E, Gazouli M, Andreadou M, Comor M, Abazovic N, Sechi LA, Ikononopoulos J: **Direct detection of unamplified DNA from pathogenic mycobacteria using DNA-derivatized gold nanoparticles.** *Journal of Microbiological Methods* 2009, **78**:260-264.
 87. Costa P, Amaro A, Botelho A, Inacio J, Baptista PV: **Gold nanoprobe assay for identification of mycobacteria from the Mycobacterium tuberculosis complex.** *Clin Microbiol Infect* 2009.
 88. Gazouli M, Liandris E, Andreadou M, Sechi LA, Masala S, Paccagnini D, Ikononopoulos J: **Specific Detection of Unamplified Mycobacterial DNA by Use of Fluorescent Semiconductor Quantum Dots and Magnetic Beads.** *J Clin Microbiol* 2010, **48**:2830-2835.
 89. Li H, Jing F, Gao Q, Jia C, Chen J, Jin Q, Zhao J: **[Membrane transfer-based colorimetric DNA detection using enzyme modified gold nanoparticles].** *Sheng Wu Gong Cheng Xue Bao* 2010, **26**:1135-1142.

90. Daniel MC, Astruc D: **Gold nanoparticles: assembly, supramolecular chemistry, quantum-size-related properties, and applications toward biology, catalysis, and nanotechnology.** *Chem Rev* 2004, **104**:293-346.
91. Boisselier E, Astruc D: **Gold nanoparticles in nanomedicine: preparations, imaging, diagnostics, therapies and toxicity.** *Chem Soc Rev* 2009, **38**:1759-1782.
92. Faraday M: **The Bakerian Lecture: Experimental Relations of Gold (and Other Metals) to Light.** *Philosophical Transactions of the Royal Society of London* 1857, **147**:145-181.
93. S.J. Oldenburg RDA, S.L. Westcott, N.J. Halas: **Nanoengineering of optical resonances.** *Chemical Physics Letters* 1998, **288**:243-247.
94. Ju-Nam Y, Lead JR: **Manufactured nanoparticles: An overview of their chemistry, interactions and potential environmental implications.** *Science of The Total Environment* 2008, **400**:396-414.
95. Sardar R, Funston AM, Mulvaney P, Murray RW: **Gold nanoparticles: past, present, and future.** *Langmuir* 2009, **25**:13840-13851.
96. Turkevich J, Stevenson P, Hillier J: **A study of the nucleation and growth processes in the synthesis of colloidal gold.** *Discuss Faraday Soc* 1951, **11**:55-75.
97. Wang Z, Ma L: **Gold nanoparticle probes.** *Coordination Chemistry Reviews* 2009, **253**:1607-1618.
98. Brust M, Walker M, Bethell D, Schiffrin DJ, Whyman R: **Synthesis of thiol-derivatised gold nanoparticles in a two-phase Liquid-Liquid system.** *Journal of the Chemical Society, Chemical Communications* 1994:801-802.
99. Ma L-N, Liu D-J, Wang Z-X: **Synthesis and Applications of Gold Nanoparticle Probes.** *Chinese Journal of Analytical Chemistry* 2010, **38**:1-7.
100. Reynolds RA, Mirkin CA, Letsinger RL: **Homogeneous, Nanoparticle-Based Quantitative Colorimetric Detection of Oligonucleotides.** *Journal of the American Chemical Society* 2000, **122**:3795-3796.
101. Zhao W, Brook MA, Li Y: **Design of Gold Nanoparticle-Based Colorimetric Biosensing Assays.** vol. 9. pp. 2363-2371: WILEY-VCH Verlag; 2008:2363-2371.
102. Li, Rothberg LJ: **Label-Free Colorimetric Detection of Specific Sequences in Genomic DNA Amplified by the Polymerase Chain Reaction.** *Journal of the American Chemical Society* 2004, **126**:10958-10961.
103. Sato K, Hosokawa K, Maeda M: **Rapid aggregation of gold nanoparticles induced by non-cross-linking DNA hybridization.** *J Am Chem Soc* 2003, **125**:8102-8103.
104. Alivisatos AP, Johnsson KP, Peng X, Wilson TE, Loweth CJ, Bruchez MP, Jr., Schultz PG: **Organization of 'nanocrystal molecules' using DNA.** *Nature* 1996, **382**:609-611.
105. Mirkin CA, Letsinger RL, Mucic RC, Storhoff JJ: **A DNA-based method for rationally assembling nanoparticles into macroscopic materials.** *Nature* 1996, **382**:607-609.
106. Atlas RM: *Handbook of microbiological media.* 3rd edn. Boca Raton, Fla.: CRC Press c2004.
107. Center BT: **Difco and BBL manual: manual of microbiological culture media.** 2nd edition: Mary Jo Zimbro, David A. Power, Sharon M. Miller, George E. Wilson, Julie A. Johnson.
108. Parish T, Stoker NG: **Mycobacteria protocols.** Totowa, N.J.: Humana Press; 1998.
109. Susan Frackman GK, Dan Simpson and Doug Storts: **Betaine and DMSO: Enhancing Agents for PCR** In *Promega Notes*: Promega.com; 1998.
110. Grabar KC, Freeman RG, Hommer MB, Natan MJ: **Preparation and Characterization of Au Colloid Monolayers.** *Analytical Chemistry* 1995, **67**:735-743.
111. Boddingtonhaus B, Rogall T, Flohr T, Blocker H, Bottger EC: **Detection and identification of mycobacteria by amplification of rRNA.** *J Clin Microbiol* 1990, **28**:1751-1759.

112. Chakravorty S, Helb D, Burday M, Connell N, Alland D: **A detailed analysis of 16S ribosomal RNA gene segments for the diagnosis of pathogenic bacteria.** *J Microbiol Methods* 2007, **69**:330-339.
113. Li H, Rothberg L: **Colorimetric detection of DNA sequences based on electrostatic interactions with unmodified gold nanoparticles.** *Proc Natl Acad Sci U S A* 2004, **101**:14036-14039.
114. Boom R, Sol CJ, Salimans MM, Jansen CL, Wertheim-van Dillen PM, van der Noordaa J: **Rapid and simple method for purification of nucleic acids.** *J Clin Microbiol* 1990, **28**:495-503.
115. Glynou K, Ioannou PC, Christopoulos TK, Syriopoulou V: **Oligonucleotide-Functionalized Gold Nanoparticles as Probes in a Dry-Reagent Strip Biosensor for DNA Analysis by Hybridization.** *Analytical Chemistry* 2003, **75**:4155-4160.
116. Shawky SM, Bald D, Azzazy HME: **Direct detection of unamplified hepatitis C virus RNA using unmodified gold nanoparticles.** *Clinical Biochemistry*, **43**:1163-1168.
117. Litos IK, Ioannou PC, Christopoulos TK, Traeger-Synodinos J, Kanavakis E: **Genotyping of Single-Nucleotide Polymorphisms by Primer Extension Reaction in a Dry-Reagent Dipstick Format.** *Analytical Chemistry* 2006, **79**:395-402.
118. Storhoff JJ, Lucas AD, Garimella V, Bao YP, Muller UR: **Homogeneous detection of unamplified genomic DNA sequences based on colorimetric scatter of gold nanoparticle probes.** *Nat Biotechnol* 2004, **22**:883-887.
119. Doria G, Franco R, Baptista P: **Nanodiagnosics: fast colorimetric method for single nucleotide polymorphism/mutation detection.** *IET Nanobiotechnol* 2007, **1**:53-57.
120. Sato K, Hosokawa K, Maeda M: **Colorimetric biosensors based on DNA-nanoparticle conjugates.** *Anal Sci* 2007, **23**:17-20.
121. Huber M, Wei TF, Muller UR, Lefebvre PA, Marla SS, Bao YP: **Gold nanoparticle probe-based gene expression analysis with unamplified total human RNA.** *Nucleic Acids Res* 2004, **32**:e137.
122. Storhoff JJ, Marla SS, Bao P, Hagenow S, Mehta H, Lucas A, Garimella V, Patno T, Buckingham W, Cork W, Muller UR: **Gold nanoparticle-based detection of genomic DNA targets on microarrays using a novel optical detection system.** *Biosens Bioelectron* 2004, **19**:875-883.
123. Bao YP, Huber M, Wei TF, Marla SS, Storhoff JJ, Muller UR: **SNP identification in unamplified human genomic DNA with gold nanoparticle probes.** *Nucleic Acids Res* 2005, **33**:e15.

